

# **LIMIT STATES FOR BAMBOO STRIPS BOLTED TO TIMBER MEMBERS**

by

Shawn LeRoy Platt

B.S. in Civil Engineering, University of Pittsburgh, 2014

Submitted to the Graduate Faculty of

Swanson School of Engineering in partial fulfillment

of the requirements for the degree of

Master of Science

University of Pittsburgh

2015

UNIVERSITY OF PITTSBURGH  
SWANSON SCHOOL OF ENGINEERING

This thesis was presented

by

Shawn LeRoy Platt

It was defended on

November 23, 2015

and approved by

John Brigham, PhD., Assistant Professor

Department of Civil and Environmental Engineering

Qiang Yu, PhD., Assistant Professor

Department of Civil and Environmental Engineering

Thesis Advisor: Kent A. Harries, PhD., Associate Professor

Department of Civil and Environmental Engineering

Copyright © by Shawn LeRoy Platt

2015

# **LIMIT STATES FOR BAMBOO STRIPS BOLTED TO TIMBER MEMBERS**

Shawn LeRoy Platt, M.S.

University of Pittsburgh, 2015

This paper presents an experimental program investigating the application of a laminated engineered bamboo strip material as an alternative means of repairing or retrofitting damaged timber structural members. This research involves the determination of characteristic properties including the open-hole tension capacity and the effects of staggered open-holes on the capacity of the engineered bamboo strip product. Limit states identified include gross and net section tension capacities, splitting and shear capacities of bolted connections and the effects of staggering bolts. The bamboo strips displayed reliable patterns of material behaviour. The application of the bamboo strip material is introduced in a pilot study repairing and reinforcing notched timber members.

## TABLE OF CONTENTS

<b>ACKNOWLEDGMENTS .....</b>	<b>X</b>
<b>NOMENCLATURE.....</b>	<b>XI</b>
<b>1.0 INTRODUCTION.....</b>	<b>1</b>
<b>1.1 LITERATURE REVIEW .....</b>	<b>4</b>
<b>1.2 EXISTING CODES AND STANDARDS.....</b>	<b>7</b>
<b>1.3 SCOPE AND OBJECTIVE OF WORK.....</b>	<b>17</b>
<b>2.0 ENGINEERED BAMBOO STRIP MATERIAL .....</b>	<b>19</b>
<b>2.1 DIRECT TENSION TESTING EXPERIMENTAL PROGRAM .....</b>	<b>19</b>
<b>2.2 ENGINEERED BAMBOO STRIP MATERIAL .....</b>	<b>20</b>
<b>2.2.1 Ultimate Capacity, <math>F_u</math> and Modulus of Elasticity, <math>E</math>.....</b>	<b>21</b>
<b>2.2.2 Shear Modulus, <math>G</math> .....</b>	<b>22</b>
<b>2.3 SUMMARY .....</b>	<b>26</b>
<b>3.0 OPEN-HOLE TENSION TESTS .....</b>	<b>27</b>
<b>3.1 TEST PROGRAM .....</b>	<b>27</b>
<b>3.1.1 Digital Image Correlation .....</b>	<b>28</b>
<b>3.2 OPEN-HOLE TEST RESULTS AND DISCUSSION.....</b>	<b>29</b>
<b>3.2.1 Effect of Stagger.....</b>	<b>31</b>
<b>3.2.2 DIC Results .....</b>	<b>32</b>
<b>3.3 SUMMARY .....</b>	<b>36</b>

<b>4.0</b>	<b>BOLTED LAP-SPLICE TENSION TESTS.....</b>	<b>38</b>
<b>4.1</b>	<b>TEST PROGRAM.....</b>	<b>38</b>
<b>4.2</b>	<b>BOLTED LAP-SPLICE TEST RESULTS AND DISCUSSION .....</b>	<b>41</b>
<b>4.2.1</b>	<b>Multiple Bolts, <math>N</math> .....</b>	<b>44</b>
<b>4.2.2</b>	<b>Leading Edge Distance, <math>L_e</math> .....</b>	<b>45</b>
<b>4.2.3</b>	<b>Longitudinal Bolt Spacing, <math>s</math> .....</b>	<b>47</b>
<b>4.2.4</b>	<b>Bolt Diameter .....</b>	<b>47</b>
<b>4.2.5</b>	<b>Effect of Stagger.....</b>	<b>48</b>
<b>4.3</b>	<b>SUMMARY .....</b>	<b>48</b>
<b>5.0</b>	<b>FLEXURAL REPAIR OF TIMBER USING BAMBOO STRIPS.....</b>	<b>50</b>
<b>5.1</b>	<b>INTRODUCTION .....</b>	<b>50</b>
<b>5.2</b>	<b>FLEXURAL TEST PROGRAM.....</b>	<b>51</b>
<b>5.2.1</b>	<b>Notched Timber .....</b>	<b>52</b>
<b>5.2.2</b>	<b>Test Specimens.....</b>	<b>53</b>
<b>5.2.3</b>	<b>Test Arrangement.....</b>	<b>54</b>
<b>5.3</b>	<b>FLEXURAL TEST RESULTS AND DISCUSSION.....</b>	<b>60</b>
<b>5.4</b>	<b>SUMMARY .....</b>	<b>64</b>
<b>6.0</b>	<b>CONCLUSIONS AND RECOMENDATIONS FOR FUTURE WORK.....</b>	<b>67</b>
	<b>APPENDIX A .....</b>	<b>70</b>
	<b>BIBLIOGRAPHY .....</b>	<b>99</b>

## LIST OF TABLES

Table 1 – Comparison of Material Properties of Bamboo, Engineered Bamboo and other Common Building Materials (adapted from B. Sharma et al. 2015, Kretschmann, D. E. 2012, Mahdavi et al. 2011 and Dixon et al. 2014).....	5
Table 2 – Average bamboo strip material properties.....	21
Table 3 – Average shear capacities.....	25
Table 4 – Open-hole specimen geometry .....	28
Table 5 – Average open-hole strength of bamboo strip having single row of holes .....	30
Table 6 – Average open-hole capacity and observed effect of hole stagger .....	32
Table 7 – Single gage bolted lap-splice specimen geometry .....	40
Table 8 – Multiple gage and staggered bolted lap-splice specimen geometry .....	40
Table 9 – Average strength of single gage bolted connections .....	43
Table 10 – Average strength of multiple gage and staggered bolted connections.....	43
Table 11 – Summary of the effect of leading edge distance and associated single bolt failure modes .....	45
Table 12 – Capacities of specimens having $N = 2$ .....	47
Table 13 – Flexural beam test arrangement.....	55
Table 14 – Single Bolt Shear Capacity Limit States.....	58
Table 15 –Bamboo Strip Tension Capacity Limit States.....	59
Table 16 Summary of beam test results.....	60

## LIST OF FIGURES

Figure 1 - Laminated bamboo orientation, radial horizontal orientation, and radial vertical orientation (Sharma et al. 2015).....	6
Figure 2 – Mechanical properties testing ASTM D143-14 .....	10
Figure 3 - Example of a flexure test for large beams with the need for lateral support (ASTM D198) .....	13
Figure 4 –Spacing of fasteners.....	16
Figure 5 – Engineered bamboo strip material.....	20
Figure 6 – Shear specimens prior to testing (redlines indicate glue lines) .....	24
Figure 7 – Observed shear failures .....	25
Figure 8 – Direct tension test.....	28
Figure 9 – Failure modes observed in open-hole tests.....	31
Figure 10 - DIC images of single 12.7 mm hole specimens.....	34
Figure 11 - DIC images of single 25.4 mm hole specimens.....	35
Figure 12 – Bolted lap-splice specimen geometry.....	39
Figure 13 – Failure modes observed in bolted tests (bolts removed in some images) .....	42
Figure 14 – Relative capacities of connections having multiple bolts.....	44
Figure 15 - Failure mode transitions.....	46
Figure 16 – Minimum leading edge and spacing criteria (12.7 mm diameter bolts).....	49
Figure 17 – Notch limitations for Sawn Lumber Beams (NDS 1997) .....	52
Figure 18 – Lumber grading .....	53
Figure 19 – End grain view showing variation in heartwood inclusion. ....	54



Figure 20 – Bolt details on notched beams .....	59
Figure 21 – Failure progression of Beam CNa .....	62
Figure 22 – Failure progression of Beam CNb .....	62
Figure 23 – Beam with color variation (Beam BNSa).....	63
Figure 24 – Beam at failure of bamboo (Beam BNa).....	64
Figure 25 – Failures of bolted bamboo strips .....	64
Figure 26 – Stress distribution .....	66

## **ACKNOWLEDGMENTS**

Projects like these are made up of many different components, all of which provide support and guidance. This support comes in many forms and is integral to a project's success. First, I would like to thank Dr. Kent Harries for not only leading the charge in this endeavor, but for being a mentor and inspiring me to push further and harder in my career. His love for all things bamboo has sparked a lifelong interest for me. I would also like to thank Charles Hager for all of his efforts in the lab for which many projects are supported by his wealth of expertise. The Watkins-Haggart Structural Engineering Laboratory has been my home away from home during this time and has provided the equipment and material to undertake this research. Additionally, I would like to thank the committee members, Dr. John Brigham and Dr. Qiang Yu, for their time and input.

I would also like to thank Logan Platt, his interest in covered bridges provided a catalyst for this investigation and his help in the lab provided a memorable experience. My family has been an unyielding support structure providing their patience and love for which I will be eternally grateful. Some of the others contributing their time and support include Janine Domingos, Elizabeth Crumley, and Tianqiao Liu.

## NOMENCLATURE

a	Distance from reaction to nearest load point, mm. (in.)
A	Cross-sectional area, mm <sup>2</sup> (in. <sup>2</sup> )
A <sub>g</sub>	Gross cross-sectional area, mm <sup>2</sup> (in. <sup>2</sup> )
A <sub>n</sub>	Net cross-sectional area, mm <sup>2</sup> (in. <sup>2</sup> )
b	Specimen width, mm (in.)
C <sub>D</sub>	Load duration factor
C <sub>M</sub>	Wet service factor
C <sub>t</sub>	Temperature factor
C <sub>L</sub>	Beam stability factor
C <sub>F</sub>	Size factor
C <sub>fu</sub>	Flat use factor
C <sub>r</sub>	Repetitive member factor
C <sub>f</sub>	Form factor
d	Specimen depth, mm (in.)
D	Diameter of bolt or lag screw, mm (in.)
E	Modulus of elasticity, MPa (ksi)
E <sub>app</sub>	Apparent modulus of elasticity, MPa (ksi)
F <sub>b</sub>	Tabulated bending fiber stress design values, MPa (ksi)

$F'_b$	Allowable bending fiber stress design values, MPa (ksi)
$F_u$	Maximum tensile stress, MPa (ksi)
$g$	Distance between rows, mm (in.)
$G$	Shear modulus, MPa (ksi)
$h$	Diameter of hole, mm (in.)
$I$	Moment of inertia of the cross section about a designated axis, $\text{mm}^4$ ( $\text{in}^4$ )
$k$	Reduction factor
$L$	Span of beam, mm (in.)
$L_c$	Leading edge distance, mm (in.)
$M$	Maximum bending moment borne by beam, N-m (lbf-in.)
$M'$	Allowable maximum bending moment borne by beam, N-m (lbf-in.)
$n$	Sample size
$N$	number of holes and/or fasteners
$P_u$	Maximum tensile load, kN (lbf)
$P'$	Allowable maximum tensile load, kN (lbf)
$P_{\max}$	Maximum load borne by beam loaded to failure, kN (lbf).
$Q$	Applied concentrated load, kN (lbf.)
$Q'$	Allowable applied concentrated load, kN (lbf.)
$s$	Center to center spacing between adjacent fasteners in a row, mm (in.)
$S$	Elastic section modulus, $\text{mm}^3$ ( $\text{in}^3$ )
$t$	Bamboo strip thickness, mm (in.)
$T_n$	Reduced open hole tensile capacity, kN (ksi)
$\alpha$	Stress reduction factor without repair

$\beta$	Stress reduction factor with repair
$\rho$	Density
$\Delta$	Deflection at midspan
$\varepsilon$	Strain

## **1.0 INTRODUCTION**

With an aging infrastructure comes a greater need for structural (i.e., load-bearing) repair and even greater need for appropriate materials, means and methods to execute those repairs. Additionally, recent interest has been redirected from traditional products to a focus on environmental concerns and sustainability. In the case of a timber-framed building or bridge, replacing a damaged timber may be impractical, costly or aesthetically unacceptable; particularly in the case of historical preservation, replacement may be prohibited. With repair being the most cost effective option in many cases, the question becomes what kind of repair and with what material? Traditionally structural repairs would be completed using a steel plate bolted and/or adhered to the damaged timber. Such a repair has some limitations and potentially adverse effects on both the fabric and performance of the structure. For the repair of an historic or architecturally sensitive structure, the use of adhesives may be prohibited as the repair must be reversible at some time in the future (United States Department of the Interior 1995). Secondly, the introduction of a material with properties that significantly differ from the parent material may result in changes in the performance of the system that could, for instance, promote or magnify damage in other areas of the system as a result of altered load paths.

In many areas, fibre reinforced polymer (FRP) composites are at the forefront of repair technology (e.g., ACI 2008). Bamboo, a material being ‘rediscovered’ due largely to its

sustainable ‘credentials’, has been used in construction for millennia and could be considered nature’s FRP. Bamboo is composed of vascular bundles consisting of longitudinal fibres bound together with a lignin matrix. The fibres are the source of bamboo’s superior mechanical properties (including tensile capacity and toughness) but also make designing with bamboo unlike designing with most conventional materials (Harries et al. 2012).

There have been many investigations into the properties of full-culm bamboo (e.g., Janssen 1981, Sharma 2010, Richard 2013). However, despite its favourable mechanical properties, the use of the full-culm bamboo in construction is limited and its use as a potential repair material impractical. Taking advantage of superior mechanical properties, bamboo has been incorporated into applications as diverse as flooring and glue-laminated members or “glubam” (Xiao et al. 2008); reinforcement for concrete and masonry (Ghavami 2005), and; reinforcing fibres for mortars and polymers (Li et al. 2011). Nonetheless, the FRP-like attributes of bamboo materials (superior, although highly anisotropic mechanical properties) has not been leveraged in many cases; this has led to our interest in the repair field.

The focus of this study is the application of manufactured bamboo strips for structural repair used in a manner similar to modern FRP methods (e.g., ACI 2008). The application envisioned is the repair of timber structures for which bamboo, it is proposed, offers an aesthetically similar or virtually invisible alternative. The comparable stiffness of bamboo and timber results in a more natural interface mitigating induced stress raisers often associated with structural repairs. The tensile strength of bamboo is generally superior to that of most species of timber, thereby not only repairing but potentially strengthening the original structure without compromising aesthetics or the architectural fabric of the structure. With an emphasis on repair of historic or architecturally sensitive structures, bolted external repairs, rather than adhesively

bonded, are preferred, since these are more easily reversed (United States Department of the Interior, 1995).

When compared to isotropic materials such as steel, bolted connections in an orthotropic material such as most FRP materials and bamboo, will redistribute stresses markedly differently. The anisotropic and relatively brittle nature of bamboo and manufactured bamboo strips render conventional assumptions of net section design inappropriate (Cunningham et al. 2015). Furthermore, even adopting guidance for conventional orthotropic materials (like FRP) is likely inappropriate since the degree of anisotropy – the ratio of longitudinal to transverse material properties – is typically much greater for bamboo.

Many studies have addressed the engineering properties of full-culm bamboo including some that have addressed the capacity of bolted connections (e.g., Janssen 1981, Sharma 2010). Arce-Villalobos (1993) found the transverse tensile modulus of elasticity of bamboo to be approximately one eighth of that measured in the longitudinal direction and concluded that “the majority of fittings based on some sort of penetration normally used in construction (nails, bolts, pegs) are not suitable for bamboo because they create high tangential stresses.” These previous studies explored the properties of full-culm bamboo; however, there remains a need to address the properties of engineered bamboo products. There is no known previous research that proposes the use of engineered bamboo as a potential repair material.



## 1.1 LITERATURE REVIEW

In an age of sustainability, construction methods must adapt. The ever-expanding modern world demands the implementation of more diverse and environmentally friendly resources to support and reinforce the construction industry. Wood construction is seeing resurgence just as older timber structures are in desperate need of repairs. With the attention of wood and wood products in the minds of architects, designers, engineers, and contractors alike, it is little wonder that there is an interest in new engineered products. The implementation of bamboo into this medium is a natural progression and provides some familiarity to the end users of the product.

Engineered construction materials have been a staple for many years with research and literature dating back to the early 1900's. The more generally termed "alternative" or "engineered lumber" contains products such as laminated veneer lumber (LVL), oriented strand lumber (OSL), and parallel strand lumber (PSL) (ASTM D3737-12). Glue-laminated lumber, or 'Glulam' is one such product that utilizes thin laminations of kiln-dried sawn lumber. This product is used for long spans that support heavy loads and in architecturally exposed systems. These engineered lumber materials come in many shapes and sizes. They provide a product that is generally more uniform and has higher strengths than sawn lumber. They may also be formed in to various shapes such as arches (Aghayere and Vigil, 2007).

Similar to wood, bamboo also takes a variety of engineered forms. With mechanical properties that typically exceed those of structural lumber and LVL, engineered bamboo members generally take one of two forms, bamboo scrimber (also known as strand-woven or parallel-strand bamboo) and laminated bamboo (which is constructed of rectangular strips) (Sharma et al. 2015). Both of these approaches are typically formed into rectangular shaped

beams or laminated bamboo lumber (LBL). Bamboo plywood and ‘GluBam’, a laminated bamboo lumber (LBL) product constructed of finger-jointed layers of bamboo laminated to form large structural girders (Xiao et al. 2008) are also commercially available engineered bamboo products. Bamboo provides several advantages over other construction materials such as strength and aesthetic appeal.

Laminated bamboo lumber (LBL) has gained popularity among practitioners due to the ability to manufacture the mechanical properties of bamboo into a more familiar product with well-defined dimensions (Mahdavi et al. 2011). An example of the mechanical properties of bamboo that may be taken advantage of can be seen in Table 1 where they are compared with some more traditional construction products.

**Table 1 – Comparison of Material Properties of Bamboo, Engineered Bamboo and other Common Building Materials (adapted from B. Sharma et al. 2015, Kretschmann, D. E. 2012, Mahdavi et al. 2011 and Dixon et al. 2014)**

Building material	Density	Tensile strength	Modulus of elasticity (MOE)	Modulus of rupture (MOR)
	(kg/m <sup>3</sup> )	MPa	GPa	MPa
Moso bamboo	630	94-194	11	130
Bamboo scrimber	600-1240	41-138	6-15	54-266
Laminated bamboo	510-980	82-191	8-23	82-144
Loblolly pine	510	80	12	88
Douglas fir	450	108	14	88
Cast iron	9670	170	190	200
Aluminum alloy	2720	270-450	69	200
Structural steel	7850	400	200	400
Carbon fiber	1760	1730	150	5650

There are numerous methods and techniques for producing engineered bamboo products and research is being conducted to investigate the potential benefits or detriments of these processes. With more than 1200 species worldwide, bamboo is widely available and a rapidly renewable sustainable resource. It's use in raw, full culm, form is limited due to its variation in geometric form as well as the difficulty in making connections. Sharma et al. (2015) investigated the production of various forms of laminated bamboo material and conducted testing on two of these: a bamboo scrimber product and laminated bamboo sheets which were then cut and processed further into a built-up member in one of two different orientations, radial horizontal and radial vertical, referring to the orientation of the original strip within the newly formed beam, as seen in Figure 1.



**Figure 1 - Laminated bamboo orientation, radial horizontal orientation, and radial vertical orientation**

**(Sharma et al. 2015)**

The use of engineered bamboo is not limited to built-up beams; other forms may take their cue from the timber industry. The introduction of the timber I-joist in recent years – having sawn timber flanges and an oriented strand board (OSB) web – is a result of the both the increase

in building demands and the impact of those demands on timber harvesting. The introduction of the engineered I-joist provides a method of significantly reducing lumber manufacturing waste.

A pilot study by Aschheim et al. (2010) utilized commercially available bamboo panels to fabricate bamboo I-joists. The joists were then used to support the roof of Santa Clara University's entry in the 2007 Solar Decathlon. During the pilot study several beams were constructed and tested. The results of the tests indicated the largest contribution to the type of failures observed resulted from the failure in the finger joints used in fabricating the tension flange. The failure occurred at the point of highest tensile stress as might be expected.

It is through pilot studies and ongoing research that advancement of engineered bamboo products is being achieved. The limitations preventing a broader acceptance of bamboo as a structural material are associated with limited public knowledge and the absence of sufficient data for adoption or integration into design codes or standards. Design and testing standards exist for full culm bamboo (ISO 2004a, 2004b, 2004c) but do not provide the foundation from which builders, engineers, and architects may use in the design of bamboo structures (Sharma et al. 2015).

## **1.2 EXISTING CODES AND STANDARDS**

The current state of codes and standards provides little guidance when considering engineered bamboo as a building or structural material. Research into the raw material is still undergoing refinement with advances being made every day. At the forefront of bamboo codes and standards is the International Organization for standardization (ISO) which has developed a

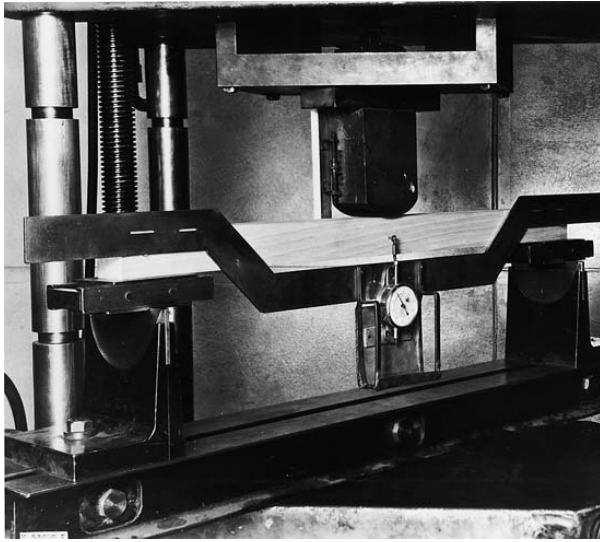
standard for material testing (ISO 2004b) and a model code for design (ISO 2004a). These are currently being revised to account for recent research and to improve their utility. While these documents provide some guidance into bamboo material characteristics, they do not address effects of the manufacturing processes involved in producing a final product in terms of a strip- or board-like material. The current application of these engineered materials as a structural material is relatively unknown, and the focus of this work.

In order to begin the process of determining the material properties and limit states of the engineered bamboo strips used in this study, several existing codes and standards were reviewed for their background and applicability to this work. Included in this background research were existing formats for wood, FRP, and some steel applications. The context of this review was to investigate the development of the standards and the methodologies used in their use as well as their integration into design codes that could then be used for design and field applications.

In the effort to better understand the bamboo strip material used in this research, a method of classifying it in terms of its mechanical properties is necessary. The use of wood standards served as a foundation from which to build a stronger and independent terminology for engineered bamboo products. There are many more bamboo species than there are wood species. The classification of wood species is done through the process of evaluating both the physical and mechanical properties of small clear specimens. The terms small and clear are relative to the wood producing industry. A small sample is one that measures 50.8 by 50.8 mm (2 by 2 in.) through its cross section having a length of 762 mm (30 in) in order to conduct a static bending test. In the event that these dimensions cannot be obtained, there is an alternate test with a smaller 25.4 mm (1 in.) square cross section and length of only 406 mm (16 in.) that is included in ASTM Standard D143-14. This smaller alternate test has limitations since the small cross

section limits the representation of the member that the specimen was taken from as well as the species as a whole. ASTM D143 provides guidance on the equipment and methods used for such tests as needed to determine capacities for compression, tension, shear, hardness, and moisture content.

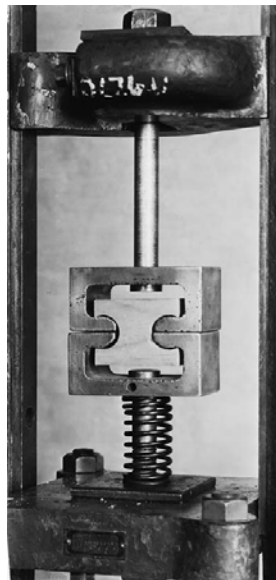
The ASTM D143 static bending test uses specimens as described above and is identical to many other standard bending tests, only differing in specimen size and loading rate. Figure 2a shows a typical set up of the bending test used in determining a wood species elastic modulus and flexure capacities. For the direct tension test, shown in Figure 2b, the specimens begin with a 25.4 by 25.4 mm (1 by 1 in.) cross section that is 457 mm (18 in.) long. The cross section is then tapered down to 9.5 by 4.8 mm (3/8 by 3/16 in.) for a length of 63.5 mm (2 ½ in.) through middle of the sample. The determination of tension capacity perpendicular to the grain is even more intricate, as seen in Figure 2c, requiring machining of the wood sample and a specialized bracket to transmit the load to the sample. When determining the shear capacity (parallel to the grain) there are several methods that have been used, ASTM D143 prescribes that shown in Figure 2d using a 50.8 by 50.8 by 63.5 mm (2 by 2 by 2 ½ in.) block which is then loaded in compressive shearing action.



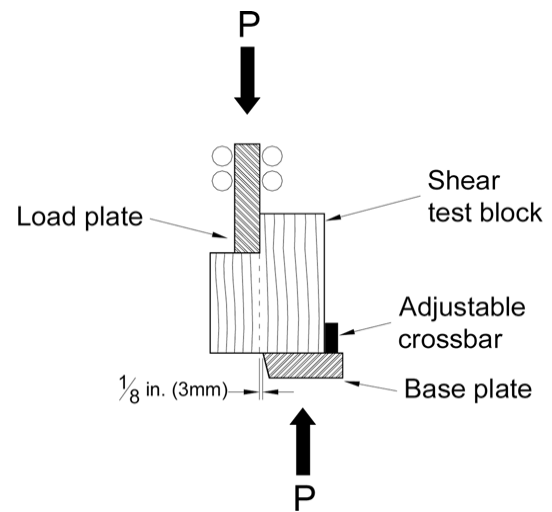
a) static bending test



b) direct tension parallel to the grain



c) tension perpendicular to the grain



d) shear test

**Figure 2 – Mechanical properties testing ASTM D143-14**

Methods presented in ASTM D143 are also used for establishing tables of strength values as reported in ASTM D2555-11. The latter document acts as a statistical base line accounting for the numerous variables affecting a species' strength including, but not limited to, harvest region, moisture content, and wood density. This data can then be utilized in formats such as the *Standard Practice for Establishing Structural Grades and Related Allowable Properties for Visually Graded Lumber* (ASTM D245-06 (2011)).

The methods presented in ASTM D143 are a staple in the wood industry and while they do not match the requirements or the physical limitations of the research being conducted here, they do provide guidance in setting standards from which to benchmark the performance of the bamboo strip material used in this research.

ASTM D245 pertains to how stress grading principles are applied for the use in establishing grades for purchase. Lumber for purchase is graded by the appropriate agencies and inspection facilities. Each piece of wood that comes off the saw has its individual characteristics such as knots, grain orientation, and location of where the member was sawn from in the original tree. These characteristics have a direct effect on the lumber's strength, utility, serviceability, and value. The need for lumber grading is in response to the variation in the defining characteristics of sawn lumber. Lumber grading generally takes one of two forms; appearance or physical, and structural or stress grades.

Visual grading is performed by thoroughly examining both ends and all four faces of the sawn lumber. Defects such as knots are located and measured. This information is used along with the stress grading to achieve a strength ratio. This ratio will help to determine a representative member's strength as a function of its moment carrying capacity in relation to a



clear specimen of the same type. The classification of stress-graded lumber is divided into four basic categories; dimension lumber, beams and stringers, posts and timbers, and stress-rated boards (ASTM D245).

This thesis pertains to dimension lumber where a rectangular section with a nominal width not exceeding 102 mm (4 in.) and nominal depth not less than 50.8 mm (2 in.; i.e. 2x4, 2x8, 4x6, etc.) are graded primarily for bending about either axis. This differs from beams and stringers only in that the minimum nominal width is 127 mm (5 in.; i.e. 6x6, 8x8, etc.) for the latter; otherwise these two classifications are identical. Some species of lumber may be further classified as dense, close, or medium grained as per section 5.6 of ASTM D245.

ASTM D198 is a set of testing methods similar to those set forth in D143 only that the context for the material is not just species identification but the evaluation of structural members with a nominal thickness equal to or greater than 32 mm (1 in.). The standard for sawn lumber was originally written in 1927 and is generally designated for bridge stringers and joists. The term structural member is one that has evolved over the decades to continuously encompass current construction methods and materials including, but not limited to, composite lumber, prefabricated I-joists, as well as newer reinforced or prestressed timbers. This is also true for the sister document ASTM D4761-13 which is the field version of the procedures given in ASTM D198. While both are acceptable, the D198 document is more focused toward establishing practices and uniform procedures. It is also the intended method for use in scientific studies.

The procedures that are given in ASTM D198 are those for use in determining flexure, compression, tension, torsion, and shear resistance. These are similar to those from D143 only on a larger scale as seen in Figure 3. This larger scale introduces more complexities within the sample itself such as the inclusion of knots and checking as well as the need to account for other

criteria in the testing such as lateral torsional buckling in flexure tests with specimens having a depth to width ratio ( $d/b$ ) greater than or equal to three. Shear modulus is also determined from a flexural test similar to that shown in Figure 3 with the exception that the load is applied as a single concentrated load placed midway between the reaction supports.

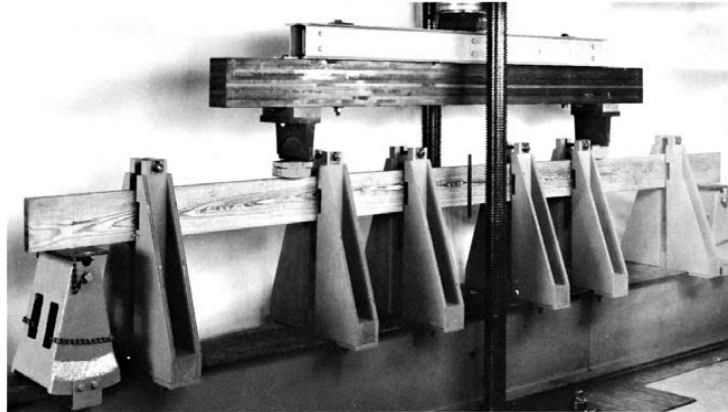


**Figure 3 - Example of a flexure test for large beams with the need for lateral support (ASTM D198)**

The tensile tests prescribed in ASTM D198 require little material preparation with the only practical limitations placed on the sample those as dictated by the testing machine. Careful attention must be given to the alignment of the grips so as to not induce any rotation or bending moment on the test specimen.

The methods promulgated by ASTM have provided guidance for further applications and standards. Included in this evolution is the American Wood Council and the *National Design Specification for Wood Construction* (NDS 1997). This document utilizes the information obtained through ASTM standards to provide a specification for the design of wood based structures.

Experimentally verified equations for critical buckling loads have been part of the NDS since 1931 (NDS 1997). These original equations were based on approximate cross sections and determined when or if the need for lateral bracing was required to mitigate lateral torsional buckling. Later research provided bending design values for slenderness factors. This research utilized 19 mm ( $\frac{3}{4}$  in.) width boards up to and including 203 mm (8 in.) depth with lengths not exceeding 508 cm (204 in.) to confirm that critical bending stresses ( $f_b$ ) could be adequately estimated with equations based on ratios of moduli of elasticity to rigidity ( $E/G$ ) equal to 16 (NDS 1997).

In 1986, after further simplifications and correlations were made between beams and columns, advances in other areas of construction allowed buckling criteria to be established for short, intermediate, and long beams. These critical buckling loads followed into the determination of the effect of notches in the beam.

In practice, the need for notching a member is quite common. These notches may be introduced to accommodate pipes or other mechanical systems, or they may be the result of some form of damage. Notches should be avoided if at all possible. This is particularly important in bending members where the notch creates a stress concentration at the corners. The process of calculating the effects of shear and parallel to the grain stresses is difficult in these regions. The 1977 edition of the NDS noted that by tapering the notch, these stresses could be reduced. Beginning with the 1944 edition, members with notches less than  $\frac{1}{6}$  of the member depth and having lengths less than  $\frac{1}{3}$  of the member depth required no special attention as they produced minimal effect on the members' stiffness. In 1977 the NDS introduced, as a result of further testing and field experience, new notch specifications. These specifications continued through the 1997 edition. The introduction of narrow slits or notches were found to introduce the

greatest amount of stress and therefore created the greatest strength reductions. These effects were reduced as the lengths of the notches were increased. The allowance of notches in lumber widths of 50.8 to 76.2 mm (2 to 3 in.) on either the compression or tension faces has proved acceptable in the outer two thirds of the member for light construction. This is in part due to the introduction of bending design values,  $F_b$ , which already include some section reductions for the inclusion of naturally occurring imperfections such as knots and checking. This allowance is not permitted for nominal dimension lumber of 102 mm (4 in.) width or greater. Notches for this size of lumber are only permitted in the tension flange at the member ends as determined by fracture mechanics as well as field experience. The beam end area, however, is susceptible to increased shear stresses making beams using this configuration more likely to split at the corners of these notches.

The design of connections between members is of particular importance in wood construction and a considerable number of failures in wood construction are a result of inadequately designed connections. The provisions for lapped joints are a form of unsymmetrical connection design where induced bending moments require special attention (NDS 1997).

Most construction designs include multiple parallel members which are loaded in compression or bending. This inherent redundancy is taken into consideration in the form of repetitive member factors,  $C_r$ , and takes into account some of the effects of load redistribution by laterally connected members such as decking and sheathing (NDS 1997). This lateral redistribution is of greater importance when considering concentrated loads such as those induced by vehicle wheels on a bridge or in a warehouse. Maximum moment and shear in bending members subject to concentrated loads are determined through the use of empirically based equations and generally provide conservative results (NDS 1997). Critical section spacing

of staggered fasteners was first introduced in the 1960 edition of the NDS. The original spacing criterion was expressed in terms of fastener spacing parallel to the grain and in the same row. This minimum spacing was 8 fastener diameters (8D). After several editions of NDS containing this parameter, it was changed in 1991 to require that staggered fasteners in adjacent rows of spacing less than 4 fastener diameters (4D) in the parallel to the grain distance be considered in the same critical section as seen in Figure 4 (NDS 1997). That is if the spacing between the staggered fasteners (parallel to the grain) was less than or equal to 4 fastener diameters (4D), those holes were considered in the same net section.

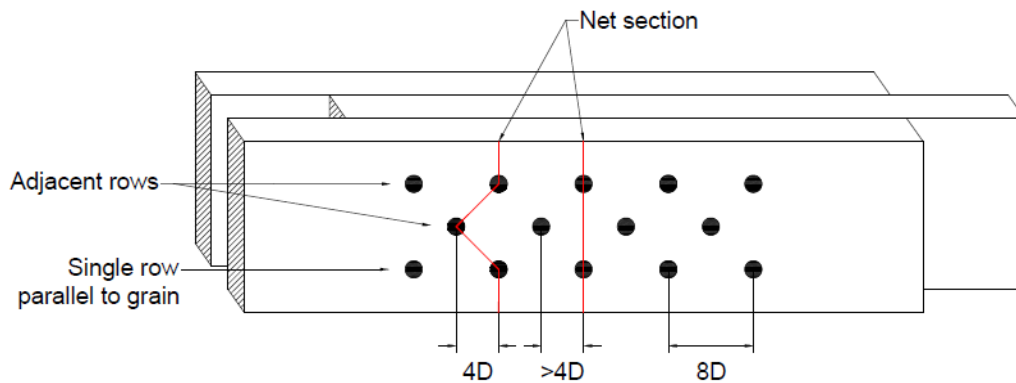


**Figure 4 –Spacing of fasteners**

The bamboo strip material used in the present research is an engineered product comprised of bamboo culm sections adhesively bound forming a board like material. A more comprehensive description of this material is discussed in Section 2.2. The composition of this product lends not only to analogies with wood in general but to wood products, specifically structural composite lumber products. ASTM provides guidance for these products in *Standard Practices for Establishing Allowable Properties for Structural Glued Laminated Timber* (ASTM

D3737-12) and *Characteristic Values for Flexural Properties of Structural Glued Laminated Timber by Full-Scale Testing* (ASTM D7341-14). While these materials have some similarities to the bamboo strip material used here, these documents are focused more towards larger members and their production. The production of the bamboo strip material is not the focus of this research, only the materials application. Nonetheless, through the reported testing, observations will be made as to potential effects of the adhesive on the test methods involved.

The use of Fiber Reinforced Polymer (FRP) standards provides a greater level of similarity with the exception that the exact composition of the bamboo is unknown. Like FRP for civil infrastructure, the engineered bamboo product is best tested as a functional unit rather than as a product with properties that are defined by the interaction of two component materials such as the bamboo fibers and lignin.

### **1.3 SCOPE AND OBJECTIVE OF WORK**

Using a limit states approach, it is necessary to address all manners by which a structure or element may fail and design for these. The focus of the current work is on bolted connections for engineered bamboo-strip repairs of timber members. The limit states of the connection include bolt shear; bearing/splitting of bamboo; shear-out of bamboo, and net section failure of bamboo. In the present work steel bolts are considered, in which case bolt shear is not a controlling limit state.

For connections requiring multiple bolts, providing a staggered bolt geometry will generally be more compact and better engage adjacent bolts by reducing the ‘shadowing’ effect

along the direction of the applied load. In isotropic materials, the effect of staggering bolts is to increase the net section tensile capacity since the failure path between adjacent staggered bolts is longer than the path across the plane net section (AISC 2010). Recent studies of the open-hole tension capacity of highly anisotropic FRP materials (Cunningham et al. 2015) concluded that the effect of stagger is reduced (compared to isotropic materials) to the point of being essentially negligible in such materials. The effect of staggered connection geometry is considered in the present study.

Chapter 2 provides a description of the engineered bamboo materials considered and experimentally determined material properties. Chapter 3 reports an experimental study investigating the open-hole tensile capacity of engineered bamboo strips. Chapter 4 then addresses the capacity of bolted lap-splice connections. The work reported in Chapters 3 and 4 has been published in the following peer-reviewed paper:

Platt, S., and Harries, K.A., Strength of Bolted Bamboo Laminate Connections, *Proceedings 15th International Conference Non-conventional Materials and Technologies* (NOCMAT 2015), Winnipeg, Canada. August 2015.

The results from the material characterization, open-hole, and bolted lap were then used to perform a pilot study, reported in Chapter 5, into the application of engineered bamboo strips to repair damaged timber flexural element. Full scale beam flexure tests on full-section as well as notched and repaired specimens were conducted.

## **2.0 ENGINEERED BAMBOO STRIP MATERIAL**

This chapter reports the fundamental tensile material properties of the engineered bamboo strip material considered and describes the tension testing protocol used for subsequent open-hole and bolted connection tests, reported in Chapters 3 and 4, respectively.

### **2.1 DIRECT TENSION TESTING EXPERIMENTAL PROGRAM**

Direct tension tests of gross section, open-hole, shear, and bolted lap-spliced specimens of engineered bamboo strip were conducted. Open-hole tests assess net section failure criteria while bolted lap-splices assess bearing, splitting and shear failures of the bamboo strips. Strain gauges were installed along the mid-line of the open hole and bolted lap-splice specimens at a location 51 mm (2 in.) from the hole furthest from the center of the specimen. This was done to investigate the strain redistribution in the specimen. A mechanical clip gauge was placed, centered vertically, on the edge of the specimens during testing (seen in Figures 5 and 7). The shear test provided a shear modulus from which to further assess the results from the other tests. All tensile tests were conducted in a servo-hydraulic 600 kN (135 kip) capacity universal test machine having hydraulic grips wider than the specimen width, ensuring uniform application of



stress at the specimen ends. Digital image correlation results (described in Section 3.2.2) confirm a uniform introduction of force to the specimens.

Direct tension tests were conducted in ‘displacement control’, specifying a rate of cross-head travel of 0.5 mm/min (0.02 in./min). This rate corresponds to a strain rate over the 203 mm (8 in.) gage length between grips of approximately 0.0025/min. For all tension tests, the number of repetitions of each test is either  $n = 3$  or  $n = 5$ .

## 2.2 ENGINEERED BAMBOO STRIP MATERIAL

Engineered Bamboo Strip Material obtained from China was used in the present study. The strips were fabricated of laminated radial-cut bamboo and have a nominal thickness of  $t = 6.4$  mm (0.25 in.) (Figure 5). Two types of strip were used: natural (two different batches) and caramelized. Caramelised strips are natural strips that have been heated in order to caramelize their lignin, thereby darkening the colour of the strip (this is done for purely aesthetic reasons). Specimens approximately 89 mm (3.5in.) wide and 406 mm (16 in.) long were cut from the supplied 203 mm (8 in.) wide strips.

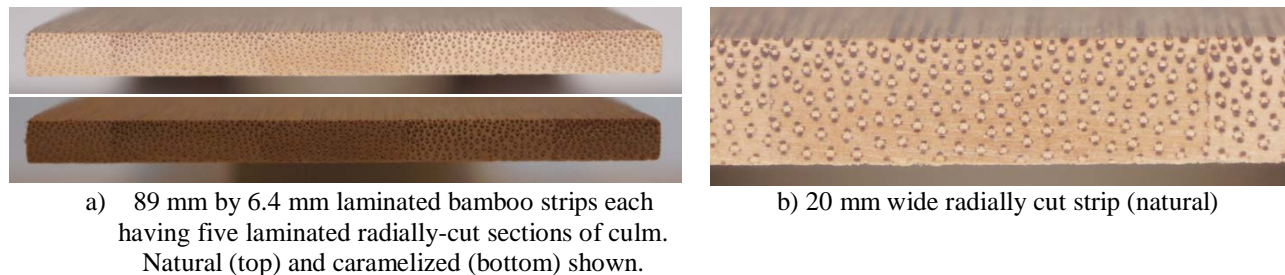


**Figure 5 – Engineered bamboo strip material**

### 2.2.1 Ultimate Capacity, $F_u$ and Modulus of Elasticity, $E$

Longitudinal (L) and transverse (T) material properties were obtained from direct tension tests of specimens having no holes as indicated in Table 2. Secant modulus of elasticity was calculated between  $0.2F_u$  and  $0.4F_u$  in all cases. As can be seen, the degree of anisotropy in terms of strength and modulus (i.e., L/T) is significant. Little difference was observed between the natural and caramelised bamboo products with the exception of the transverse tension strength ( $F_{uT}$ ) which was notably lower in the caramelised specimens. This is an indication that the caramelisation process adversely affects the lignin matrix but not the bamboo fibres. This result is mirrored in the determination of the modulus,  $E$ .

**Table 2 – Average bamboo strip material properties**

test specimens	material	orientation	n	max. load, $P_u$	max. stress, $F_u$	$F_{uL}/F_{uT}$	modulus, $E$	$E_L/E_T$
				kN (COV)	MPa (COV)		MPa (COV)	
<b>Batch 1:</b> open hole (Tables 4 & 5) and single gage bolted (Table 9)	natural	L	8	52.9 (0.11)	94.9 (0.11)	14.0	10176 (0.08)	11.6
		T	5	1.71 (0.11)	6.79 (0.11)		874 (0.20)	
	caramelised	L	5	51.7 (0.14)	92.5 (0.12)	22.8	8746 (0.14)	7.9
		T	5	1.77 (0.14)	4.06 (0.15)		1114 (0.25)	
<b>Batch 2:</b> multiple gage and staggered bolted (Table 10), shear specimens (Table 3), and beam testing (Table 16)	natural	L	5	52.0 (0.12)	91.8 (0.12)	11.7	9640 ( $<0.01$ )	6.9
		T	5	3.67 (0.10)	7.83 (0.10)		1403 (0.09)	

### 2.2.2 Shear Modulus, G

The determination of the shear modulus for the laminated bamboo strip material used in this research is necessary in understanding and developing limit states. Previous research has very little reporting of shear modulus and most available data was from outdated sources or from full culm bamboo.

In order to understand longitudinal shear behavior, the material construction must be considered. Any given section or area of this strip material may include nodal portions of the culm, varying degrees of fiber density, and the inclusion of the laminating glue line (see Figure 5). The fiber density variation is minimal across the width of the strip but, due to the radial-cut bamboo, is evident through the thickness. Considering the limit states of interest, the shear for this product will only be considered across its width of the strip and parallel to the fibers; no consideration of through-thickness shear is considered.

Shear modulus testing was accomplished using a modified version of ASTM D3846-08 (2015) *Standard Test Method for In-Plane Shear Strength of Reinforced Plastics*. All shear specimens were from “Batch 2” (see Table 2).

Using an initial specimen width of 20 mm (0.80 in) and a length of 250 mm (9.8 in), the specimens were notched from opposite sides to the midpoint of the specimen, a length of 10 mm (0.4 in.). The notches were placed with a gauge length (the distance between the notches) of 80 mm (3.15 in.). The gauge length was determined based on the necessity to accommodate the strain transducer as seen in Figure 6d.

Following initial testing, it was determined that the resulting failures were indicative of a mixed mode type failure, rather than the intended Mode II shear. This produced ultimate shear strength and modulus results lower than the characteristic Mode II behavior of interest.

New sample geometries were then produced by incrementally increasing the width of the central gage length. The gripped ends were only increased to 25 mm (1 in.) which was the maximum width allowable by the machined grips used. These grips, designed for similar FRP shear tests, were designed so that the small specimens can be anchored in the testing machine without inducing any compression forces during this phase (Cardoso 2014).

With each increase in width of the gauge length, the mixed mode failures became less evident resulting in a nearly pure Mode II failure. Along with the increase in width of the sample, the kerf of the notch was decreased by using a thinner blade to form the notch. The notch width decreased from 4 mm (0.16 in.) using a table saw to 1 mm (0.04 in.) using a scroll saw. This helped to reduce the bending (leading to a Mode I component along the shear plane) created by the larger notch.

The final specimen arrangement was determined to be 50.0 mm wide and 6.30 mm thick (2 by 0.25 in.) with 25 mm (1 in.) notches placed 79.6 mm (3.13 in.) apart. The ends of the notches terminated at the center of the specimen (see Figure 6a). Specimens were intentionally created so that the shear plane along the centerline was either located within a 20 mm bamboo width or along a glue line (see Figure 6b and 6c). Figure 6d displays the specimens prior to testing for the mid culm samples. Figure 7 shows the resulting failure planes of all specimens. The resulting secant shear modulus was calculated between  $0.2\tau_u$  and  $0.4\tau_u$  as indicated in Table 3. It is seen that glue line is the ‘weak link’ in terms of the shear capacity of the strip. The shear

modulus of the entire strip, however, will be governed by the bamboo behaviour as this comprises most of the section area. Interestingly, the presence of the glue line does affect the characteristic shear strength of the bamboo (when defined as mean minus three standard deviations) which 5.5 MPa in either case.

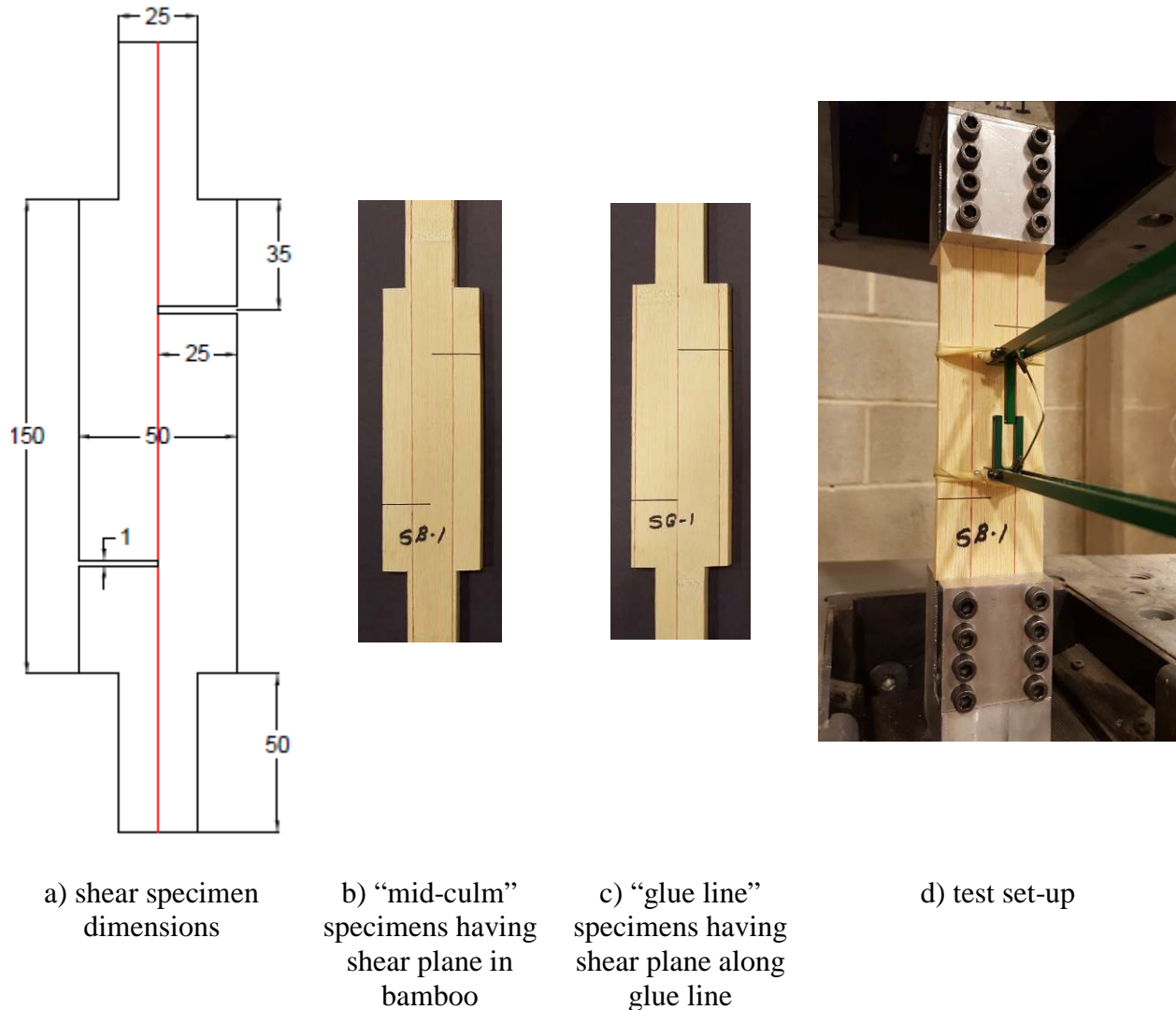
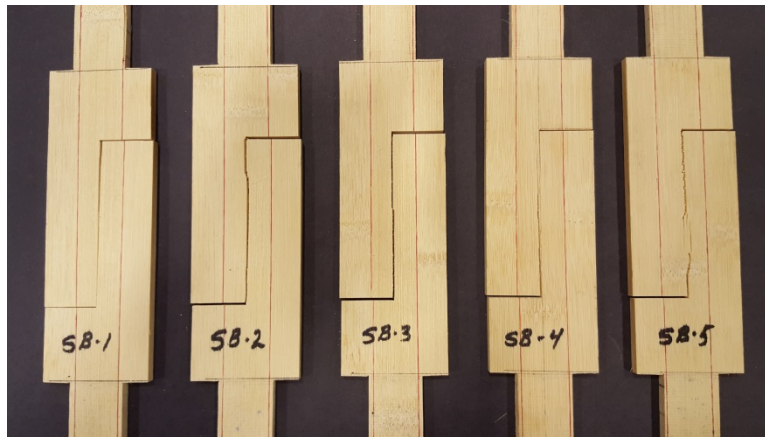
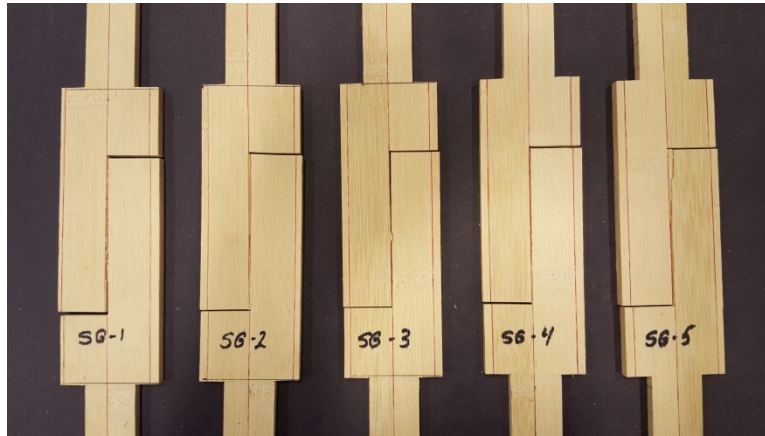


**Figure 6 – Shear specimens prior to testing (redlines indicate glue lines)**



a) failed mid culm specimens



b) failed glue line specimens

**Figure 7 – Observed shear failures**

**Table 3 – Average shear capacities**

test specimens	n	max shear stress, $\tau_u$	modulus, G
		MPa (COV)	MPa (COV)
Culm section mid line	5	7.39 (0.13)	2787 (0.13)
Glue line	5	6.67 (0.06)	3346 (0.09)

## 2.3 SUMMARY

Three batches of the bamboo strip material obtained from the same source were used in this study. Some variation of material properties was seen between these and a significant loss of lignin-dominated transverse properties was observed for the caramelised version of the material. As a result, it is recommended that only the natural form of the strips be used in structural applications.

A method for determining longitudinal shear capacity and modulus based on ASTM D3846 was demonstrated. Specimens that were too thin and larger notch kerfs introduced some Mode I behaviour along the shear plane. The combinations of 50 mm wide specimens having 1 mm kerf notches appeared to mitigate this issue.

### **3.0 OPEN-HOLE TENSION TESTS**

#### **3.1 TEST PROGRAM**

Thirteen open-hole geometries (labelled OA-ON) were tested as shown in Table 4. Each consisting of 3 to 5 specimens (sample size,  $n$ ). Specimens had from 0 to 3 holes ( $N$ ) having a diameter ( $h$ ) of 12.7 mm (0.5 in.) or 25.4 mm (1.0 in.) with spacing ( $s$ ) and gages ( $g$ ) ranging from 0 to 51 mm (0 to 2.0 in.). Due to material availability, not every geometry was tested with both materials. A typical specimen having 3-12.7 mm (0.5 in.) holes at a gage of 25.4 mm (1.0 in.) is shown in Figure 8a. All holes were drilled with a ‘brad’ bit in order to minimize damage to the bamboo strip around the hole circumference.

Strain gauges were installed along the mid-line of the open hole specimens at a location 51 mm (2 in.) from the hole furthest from the center of the specimen. A mechanical clip gauge was placed, centered vertically, on the edge of the specimens during testing (seen in Figures 8).



**Table 4 – Open-hole specimen geometry**

geometry	A	OB	OC	OD	OE	OF	OG	OH	OJ	OK	OL	OM	ON
$N$	0	1	2	2	2	2	2	2	3	3	3	3	3
$g$ (mm.)	-	-	25.4	50.8	25.4	50.8	50.8	25.4	25.4	12.7	25.4	12.7	25.4
$s$ (mm)	-	-	-	-	50.8	50.8	25.4	25.4	-	25.4	25.4	50.8	50.8



a) 89 mm wide open-hole specimen having 3-12.7 mm holes at a gage,  $g = 25.4$  mm



b) 89 mm wide bolted lap splice specimen having 2-12.7 mm bolts at a spacing,  $s = 50.8$  mm

**Figure 8 – Direct tension test**

### 3.1.1 Digital Image Correlation

Selected open-single hole samples of the laminated bamboo strip along with samples of GFRP and mild steel having similar section sizes (6.4 by 102 mm) (0.25 by 4 in.), were tested using digital image correlation (DIC) to capture the strain field in the vicinity of the hole. The different materials permit investigation of the effect of the ratio of longitudinal to transverse

material properties. The commercially available VIC-3D system (Correlated Solutions 2013) was used. A high-contrast speckle pattern of black on a white background was applied to all samples using spray paint. The DIC system calculates the strain fields by correlating consecutive images taken by a two-camera system. The displacement field of the speckle pattern is numerically processed to calculate the full strain field.

### 3.2 OPEN-HOLE TEST RESULTS AND DISCUSSION

Specimens tested having only a single row of holes (i.e.  $s = 0$ ) demonstrated some reduction in open-hole tensile capacity ( $T_n$ ) beyond the calculated effect of net section area ( $A_n = A_g - Nht$ ) as described by the factor  $k$  in Eq. 3.1. This is an indication of the stress-concentrating effect of the holes.

$$T_n = kF_{uL}(A_g - Nht) \quad (3.1)$$

In which  $F_{uL}$  is the nominal (no-hole) longitudinal tensile capacity given in Table 2,  $A_g$  is the gross cross section area and  $Nht$  is the area represented by  $N$  holes of diameter  $h$  through the strip thickness  $t$ .

As shown in Table 5, for the natural bamboo material, the observed open-hole strength reduction was near unity for 12.7 mm (0.5 in.) diameter holes and  $k \approx 0.8$  for 25 mm (1.0 in.) holes. The value of  $k \approx 0.9$  for 12.7 mm (0.5 in.) holes in the caramelized material. These values

of  $k$  are greater than comparable values observed in GFRP materials (Cunningham et al. 2015) as may be expected due to the greater degree of anisotropy in the bamboo.

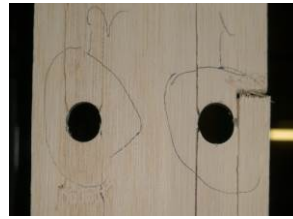
**Table 5 – Average open-hole strength of bamboo strip having single row of holes**

geometry	$N$	$h$	$g$	natural material				caramelised material			
				max. load, $P_u$	max. stress, $F_u$	strength reduction, $k$	failure mode	max. load, $P_u$	max. stress, $F_u$	strength reduction, $k$	failure mode
		mm	mm	kN (COV)	MPa (COV)	$F_u/F_{u, N=0}^a$		kN (COV)	MPa (COV)	$F_u/F_{u, N=0}^a$	
A	0	12.7	-	52.9 (0.11)	94.9 (0.11)	-	-	51.7 (0.14)	92.5 (0.12)	-	
OB	1	12.7	-	40.9 (0.11)	85.6 (0.10)	0.90	I-a	37.6 (0.12)	80.7 (0.13)	0.87	I-b
OC	2	12.7	25.4	39.9 (0.12)	99.7 (0.05)	1.05	I-a	32.3 (0.05)	83.8 (0.06)	0.91	I-c
OD	2	12.7	50.8	35.6 (0.05)	90.0 (0.05)	0.95	I-b	30.2 (0.17)	77.8 (0.17)	0.84	I-b
OJ	3	12.7	25.4	31.5 (0.07)	98.0 (0.07)	1.03	I-c	26.6 (0.21)	84.1 (0.22)	0.91	I-d
OB	1	25.4	-	29.5 (0.18)	73.8 (0.17)	0.78	I-a	-	-	-	-
OD	2	25.4	50.8	18.8 (0.18)	78.9 (0.10)	0.83	I-b	-	-	-	-
<sup>a</sup> normalised by geometry A n = 5 for all specimens except: caramelised OB, n = 3; OC, n = 4											

Failure modes observed for open-hole specimens are shown in Figure 9. These were a combination of shear (Type I-a) and splitting (Type I-b) for one and two holes. When a third hole is introduced, the net area is reduced to the point where net section rupture (Type I-c) is observed. For the caramelised material having a notably lower transverse strength, multiple longitudinal shear planes formed (Type I-d).



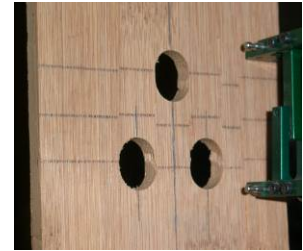
**Type I-a:** shear rupture emanating from hole



**Type I-b:** longitudinal splitting



**Type I-c:** net section fracture



**Type I-d:** longitudinal splitting of staggered hole arrangements (note initially continuous horizontal lines)

**Figure 9 – Failure modes observed in open-hole tests**

### 3.2.1 Effect of Stagger

Table 6 shows results from cases in which staggered hole lines were tested. Only 12.7 mm (0.5 in.) diameter holes were considered and, due to limited material availability, only caramelized materials were tested (Table 2). For the case of a staggered connection, the stress,  $F_u$ , is calculated based on a plane net section accounting for all holes across the section (i.e.,  $A_n = A_g - Nht$ ) regardless of stagger spacing ( $s$ ). Longitudinal splitting failures (Types I-b and I-d shown in Figure 8) dominated the staggered open-hole behaviour.

**Table 6 – Average open-hole capacity and observed effect of hole stagger**

geometry	N	g	s	c-to-c	max. load, $P_u$	max. stress, $F_u$	effect of stagger	Failure type
		mm	mm	mm	kN (COV)	MPa (COV)	$F_u/F_{u,s=0}$ <sup>a</sup>	
OC	2	25.4	-	-	32.3 (0.05)	83.8 (0.06)	-	I-b
OD	2	50.8	-	-	30.2 (0.17)	77.8 (0.17)	-	I-b
OE	2	25.4	50.8	56.8	36.5 (0.10)	93.6 (0.10)	1.12	I-b
OF	2	50.8	50.8	71.8	33.7 (0.04)	85.2 (0.05)	1.10	I-b
OG	2	50.8	25.4	56.8	34.2 (0.13)	87.0 (0.12)	1.12	I-b
OH	2	25.4	25.4	35.9	31.1 (0.05)	80.7 (0.04)	0.96	I-b
OJ	3	25.4	-	-	26.6 (0.21)	84.1 (0.22)	-	I-c
OK	3	12.7	25.4	28.4	21.8 (0.06)	70.6 (0.06)	0.84 <sup>b</sup>	I-d
OL	3	25.4	25.4	35.9	25.0 (0.14)	81.8 (0.13)	0.97	I-d
OM	3	12.7	50.8	52.4	26.5 (0.07)	84.4 (0.07)	1.00 <sup>b</sup>	I-d
ON	3	25.4	50.8	56.8	31.7 (0.05)	101 (0.05)	1.20	I-d
<sup>a</sup> normalised by geometry OC, OD or OJ having same value of g								
<sup>b</sup> normalized by geometry OJ having g = 25								
n=5 for all specimens								

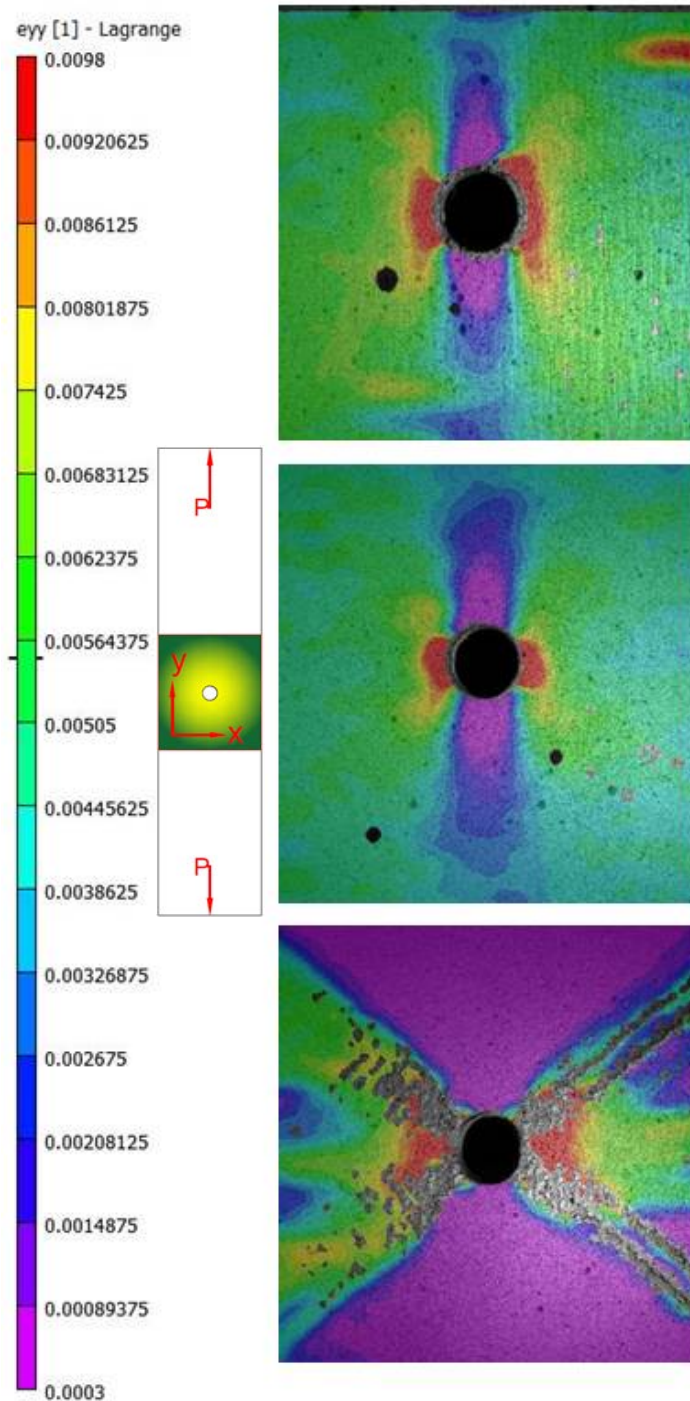
While the results of this pilot study are not conclusive, providing a stagger is observed to increase the open-hole capacity marginally provided adequate spacing between the holes is provided. Providing a diagonal center-to-center distance (c-to-c, in Table 6) of more than 51 mm (2.0 in.; 4 hole diameters) resulted in an increase in net section strength. Below 51 mm (2.0 in.), interaction between stress concentrations developed at the holes is believed to occur resulting in a reduction in net section capacity. Further study is required to verify and quantify this effect

### 3.2.2 DIC Results

Open-hole samples of the 6.4 by 102 mm (0.25 by 4.0 in.) laminated bamboo strip material along with samples of GFRP plate and mild steel all having centered 12.7 mm (0.5 in.) and 25.4 mm (1.0 in.) holes were tested in direct tension while using digital image correlation (DIC) to obtain the longitudinal strain field. Figures 10 and 11 provide the tested mechanical

properties for the GFRP and steel specimens and display representative strain field patterns for 12.7 mm (0.5 in.) holes and 25.4 mm (1.0 in.) holes, respectively. The materials presented have significant differences in their ratios of longitudinal to transverse modulus ( $E_L/E_T$ ). The ratio for the laminated bamboo used in this study ranged from 6.9 to 11.6. This is quite different from GFRP and steel which have ratios of approximately 3.1 (Cunningham et al. 2015) and 1 respectively.

The images display classic  $45^\circ$  shear behavior (12.7 mm hole in steel) for an orthotropic material. This behavior transitions to transverse-oriented cracking (25.4 mm hole in steel) with the reduction in cross sectional area by the increase in hole diameter for the same gross cross section. As the degree of anisotropy increases to from orthotropic such as FRP having an  $E_L/E_T$  ratio equal to 3.1 the images continue to show evidence of  $45^\circ$  shear behavior in the form of two ‘ears’ of high stress emanating from hole (more evident at higher stress shown in Figure 11). For a material such as the highly anisotropic bamboo strip ( $E_L/E_T = 6.9$ ) the images show little  $45^\circ$  shear behavior. Behavior is longitudinally-oriented shear, resulting in pull-out failure as described by failure Type 1-b (Figure 8).



a) bamboo strip (Batch 2)

$E_L/E_T = 6.9$

sample maximum stress,  $F_u = 80$  MPa

image at left,  $F = 0.71F_u = 56.7$  MPa

b) 6.4 mm FRP strip

$E_L/E_T = 3.1$  (Cunningham et al. 2015)

sample maximum stress,  $F_u = 363$  MPa

image at left,  $F = 0.53F_u = 194$  MPa

b) 6.4 mm steel plate

$E_L/E_T = 1$

sample maximum stress,  $F_u = 420$  MPa

image at left,  $F = 0.53F_u = 290$  MPa

Figure 10 - DIC images of single 12.7 mm hole specimens

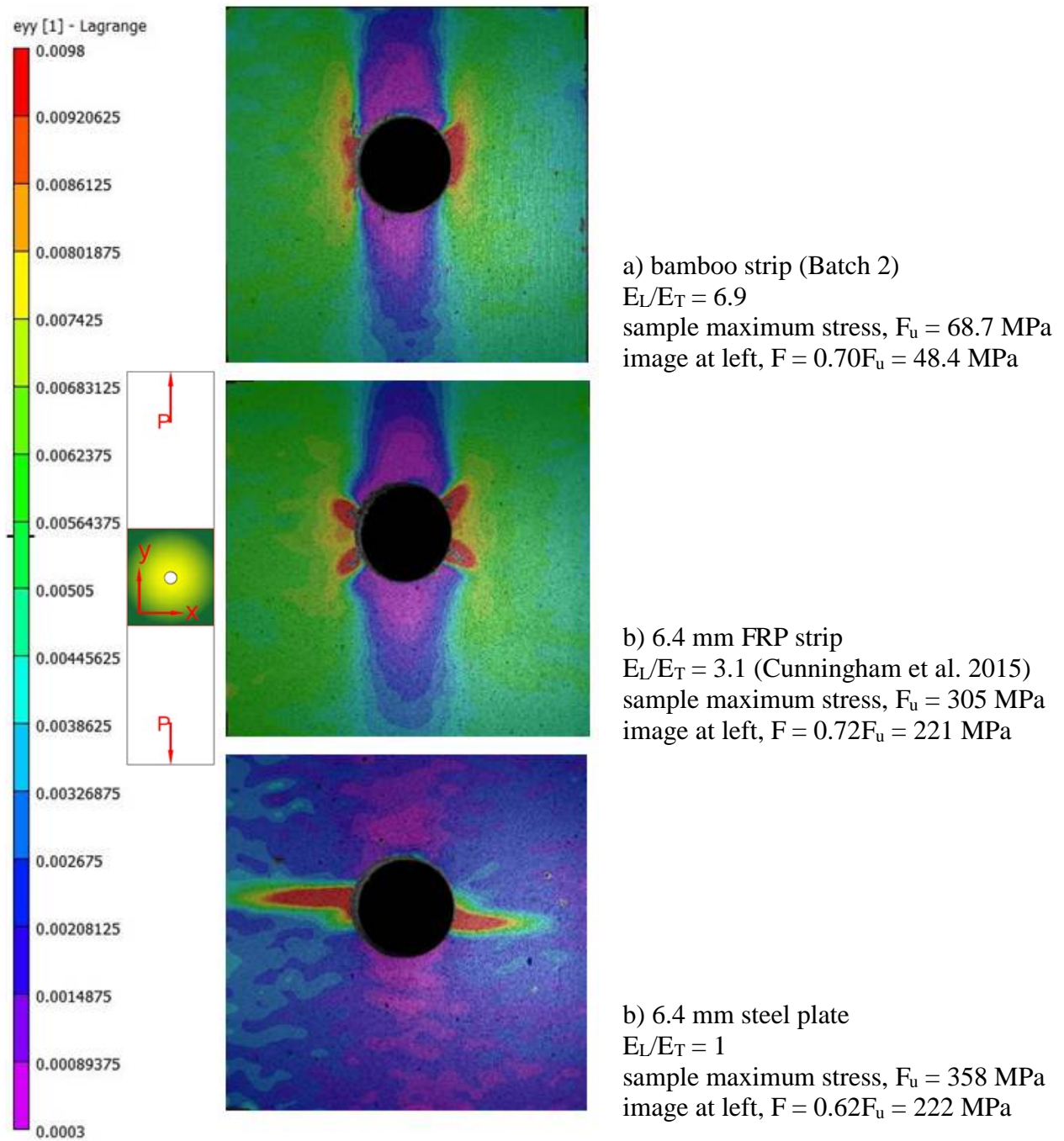


Figure 11 - DIC images of single 25.4 mm hole specimens



### 3.3 SUMMARY

Open-hole tests of engineered bamboo strips displayed reliable patterns of material behaviour. Net section reduction factors accounting for the stress-raising effect of the holes were identified to be a function of hole diameter and material anisotropy (Table 5). While no net section reduction was observed for 12.7 mm (0.5 in.) holes in 89 mm (3.5 in.) wide specimens, a reduction factor of 0.8 was observed for 25.4 mm (1.0 in.) holes in the same material. A reduction of 0.9 was observed for 12.7 mm (0.5 in.) holes in a caramelised material in which the transverse material properties are proportionally lower resulting in much greater degree of anisotropy of  $E_L/E_T = 7.9$  and  $F_{uL}/F_{uT} = 22.8$  (Table 2).

The impact of staggering the holes was observed to depend on the spacing between holes. Additional study is necessary to quantify these effects since the effect of introducing the hole is detrimental (Table 5), while the effect of staggering the holes may counteract this effect to a small degree (Table 6).

The DIC testing illustrates that as the degree of anisotropy varies, the ability of the material to effectively ‘channel’ stress around holes is affected. With increasing anisotropy, the behaviour transitions from one of 45° shear-dominated stresses leading to a transverse crack emanating from the hole – a classic net section failure observed in steel – to a behaviour characterised by longitudinal shear stresses. This behaviour will affect bolted connection design of bamboo strips in at least the following ways:

1. The shear-out limit state will likely dominate over net section behaviour.
2. The beneficial effects of staggering bolt holts in orthotropic materials will likely not be realised

3. Multiple bolts along the same gage line may become proportionally less effective.

These effects will be investigated in the following chapter.

## **4.0 BOLTED LAP-SPLICE TENSION TESTS**

### **4.1 TEST PROGRAM**

Bolted Lap-splice Specimens consisted of two 89 x 6.4 mm (3.5 x 0.25 in.) strips bolted together as shown in Figure 12. Two different batches of natural strips (Table 2) were used. Spacers were provided at each grip location to maintain a concentric load application along the lap-splice faying surface (Figure 12a).

ASTM A307 Grade A bolts (tensile strength = 414 MPa (60ksi) having a nominal diameter of 12.7 mm (0.5 in) (measured diameter of 12.4 mm (0.49 in.)) were used. The shear capacity of one bolt exceeds the tension capacity of the 89 x 6.4 mm (3.5 x 0.25 in.) bamboo strips; thus bolt shear is not a limit state of concern. Although the same bolt was used for all tests, two hole diameters ( $h$ ) were used: 12.7 and 25.4 mm (0.5 and 1.0 in.). All holes were drilled with a ‘brad’ bit in order to minimize damage to the bamboo strip around the hole circumference. The bolts were inserted directly into the 12.7 mm (0.5 in.) holes while steel sleeves having 25.4 mm (1.0 in.) OD and 12.7 mm (0.5 in.) ID were used in the 25.4 mm (1.0 in.) holes as shown in Figures 12b and c, respectively. The sleeves were machined such that they were 12.7 mm (0.5 in.) long and did not protrude beyond the lapped bamboo strips (ensuring that the washers provided clamping force to the bamboo and not the steel sleeve). The sleeves provide a larger bearing area against the bamboo without the need of providing a larger bolt.

Washers having 35 mm (1.4 in.) OD (single gage B-specimens) or 25 mm (1.0 in.) OD (multiple gage S-specimens) were installed under both the bolt head and nut. All bolts were tightened only ‘finger tight’ so as to not crush the bamboo through its thickness.

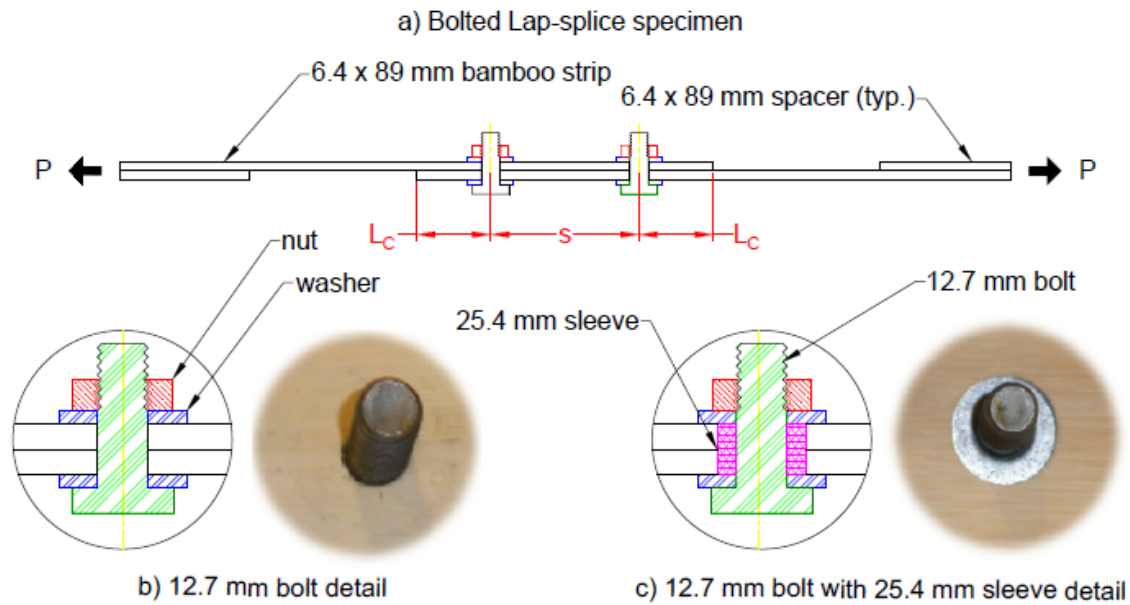


**Figure 12 – Bolted lap-splice specimen geometry**

Thirteen geometries (BB-BP), shown in Table 7, having a single gage line of from 1 to 6 bolts ( $N$ ) and spacing ( $s$ ) and edge distances ( $L_c$ ) ranging from 51 to 152 mm (2.0 to 6.0 in.) were tested. All single gage specimens were fabricated with natural bamboo strips from Batch 1 (Table 2) except BP which was from Batch 2. A typical specimen having two 12.7 mm (0.5 in.) bolts at a spacing of 50.8 mm (2.0 in.) is shown in Figure 8b.

Similar to the open-hole geometries considered, nine geometries (SB-SK), shown in Table 8, of bolted lap-splice having from 1 to 3 bolts ( $N$ ), gages ( $g$ ) of 25.4 or 38.1 mm (1.0 or 1.5 in.) and spacing ( $s$ ) ranging from 25.4 to 76.2 mm (1.0 to 3.0 in.) were considered. The edge

distance ( $L_c$ ) for all S-geometry specimens was constant at 102 mm (4.0 in.). All S-geometry specimens were fabricated with natural bamboo strips from Batch 2 (Table 1).

**Table 7 – Single gage bolted lap-splice specimen geometry**

geometry	<b>A</b>	<b>BB</b>	<b>BC</b>	<b>BD</b>	<b>BE</b>	<b>BF</b>	<b>BG</b>	<b>BH</b>	<b>BJ</b>	<b>BK</b>	<b>BL</b>	<b>BM</b>	<b>BN</b>	<b>BP</b>
$N$	0	1	1	1	2	2	2	2	3	3	4	5	5	6
$s$ (mm)	-	-	-	-	50.8	102	102	152	50.8	102	50.8	50.8	102	50.8
$L_c$ (mm)	-	50.8	102	152	50.8	102	50.8	50.8	50.8	102	50.8	50.8	102	50.8

**Table 8 – Multiple gage and staggered bolted lap-splice specimen geometry**

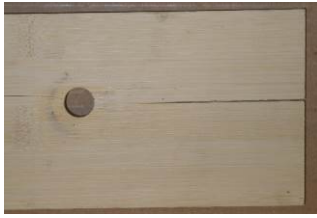
geometry	<b>A</b>	<b>SB</b>	<b>SC</b>	<b>SD</b>	<b>SE</b>	<b>SF</b>	<b>SG</b>	<b>SH</b>	<b>SJ</b>	<b>SK</b>
$N$	0	1	2	2	3	3	3	3	3	3
$g$ (mm.)	-	-	25.4	38.1	25.4	25.4	25.4	25.4	25.4	25.4
$s$ (mm)	-	-	-	-	-	25.4	38.1	50.8	63.5	76.2
$L_c$ (mm)	-	102	102	102	102	102	102	102	102	102

## **4.2 BOLTED LAP-SPLICE TEST RESULTS AND DISCUSSION**

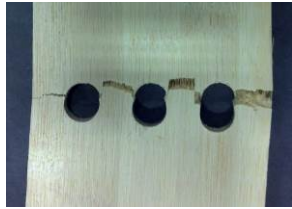
Figure 13 identifies and provides examples of the range of failure modes observed in the bolted lap-splice tests. In some cases, the change of failure mode with varying parameters helps to identify the limit states of the connection as is discussed in the following sections.

Table 9 summarises the capacities of the single gage bolted connections described in Table 7 while Table 10 summarises the capacities of the multiple gage and staggered bolt connection tests described in Table 8.

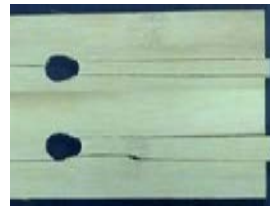
Significantly, no bolted tests approached the capacity of the bamboo strips (reported as geometry A in each table. Net section rupture (failure Type III, Figure 15) was only observed in a few cases and typically only in cases where multiple bolts increased the capacity of the connection.



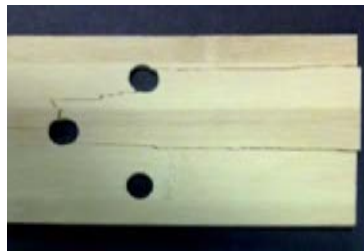
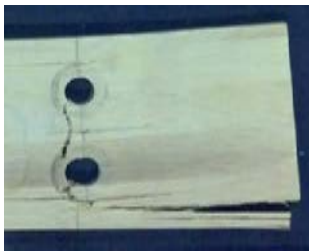
**Type II:** longitudinal splitting of bolted connection (three examples shown)



**Type III:** net section  
rupture of bolted  
connection



**Type IV:** Shear-out failure of bolted connection (three examples shown)



**Type V:** block shear of bolted connection (three examples shown)



**Type VI:** bamboo crushing ("plowing")



**Type VII:** pull-through

**Figure 13 – Failure modes observed in bolted tests (bolts removed in some images)**

**Table 9 – Average strength of single gage bolted connections**

geometry	N	<i>h</i>	<i>s</i>	<i>L<sub>c</sub></i>	max. load, <i>P<sub>u</sub></i>	multiple of single bolt capacity	failure modes
		mm	mm	mm	kN (COV)	$P_u/P_{u, s=0}^b$	
A	0	-	-	-	52.9(0.11)	-	-
BB	1	12.7	-	50.8	6.92 (0.07)	-	IV
BC	1	12.7	-	102	7.83 (0.06)	1.13	II, IV
BD	1	12.7	-	152	8.67 (0.05)	1.25	II, VI
BE	2	12.7	50.8	50.8	10.7 (0.15)	1.55	II
BF	2	12.7	102	102	13.5 (0.01)	1.72	IV
BG	2	12.7	102	50.8	15.8 (0.03)	2.28	IV
BH	2	12.7	152	50.8	14.1 (0.07)	2.04	IV
BJ	3	12.7	50.8	50.8	18.1 (0.10)	2.62	III
BK	3	12.7	102	102	23.9 (0.05)	3.05	IV
BL	4	12.7	50.8	50.8	23.8 (0.10)	3.44	IV
BM	5	12.7	50.8	50.8	30.2 (0.05)	4.36	IV, III
BP	5	12.7	102	102	30.2 (0.03)	3.86	IV
BN	6	12.7	50.8	50.8	28.9 (0.22)	4.18	III
BB	1	25.4	-	50.8	6.04 (0.24)	-	IV
BC	1	25.4	-	102	8.43 (0.12)	1.40	II, VII
BE	2	25.4	25.4	50.8	12.5 (0.05)	2.07	IV
<sup>a</sup> normalized by geometry BB ( <i>N</i> = 1) having same value of <i>L<sub>c</sub></i> and <i>h</i> n=3 for all specimens							

**Table 10 – Average strength of multiple gage and staggered bolted connections**

geometry	N	<i>h</i>	<i>g</i>	<i>s</i>	c-to-c	max. load, <i>P<sub>u</sub></i>	multiple of single bolt capacity	effect of stagger	failure modes
		mm	mm	mm	mm	kN (COV)	$P_u/P_{u, N=1}^a$		
A	0	12.7	-	-	-	51.7 (0.12)	-	-	
SB	1	12.7	-	-	-	7.22 (0.06)	-	-	IV
SC	2	12.7	25.4	-	-	14.1 (0.07)	1.95	-	IV, V
SD	2	12.7	38.1	-	-	13.8 (0.01)	1.91	-	II, IV, V
SE	3	12.7	25.4	-	-	17.9 (0.02)	2.48	-	III
SF	3	12.7	25.4	25.4	35.9	18.6 (0.17)	2.57	1.04	V
SG	3	12.7	25.4	38.1	45.8	21.6 (0.06)	2.99	1.21	II, IV, V
SH	3	12.7	25.4	50.8	56.8	22.8 (0.06)	3.16	1.27	IV, V
SJ	3	12.7	25.4	63.5	68.4	21.3 (0.10)	2.95	1.19	II
SK	3	12.7	25.4	76.2	80.3	20.7 (0.05)	2.87	1.16	II
<sup>a</sup> normalized by geometry SB having <i>N</i> = 1 <sup>b</sup> normalised by geometry SE having <i>s</i> = 0 n=3 for all specimens									



### 4.2.1 Multiple Bolts, $N$

For isotropic ductile materials such as steel, the capacity of a bolted connection is the sum of the critical limit state capacities of the individual bolts. Essentially, all bolts in a connection are assumed to resist connection forces equally. This is not the case for anisotropic and/or non-ductile materials such the bamboo strips tested in this study. As shown in Tables 9 and 10, there is a reduction associated with the capacity of multiple bolt connections. As shown in Figure 14, for  $N \leq 5$  bolts, the capacity of the bolted connection,  $P_u$ , is well represented by:

$$P_u = 0.85NP_{ul} \quad (4.2)$$

In which  $P_{ul}$  is the capacity of a single bolt (geometry BB, BC or SB) regardless of other connection parameters.

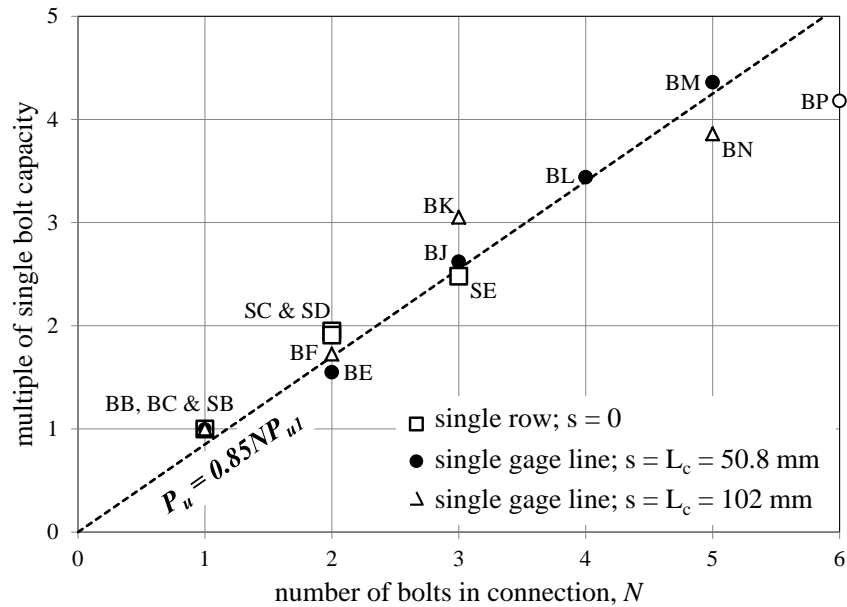


**Figure 14 – Relative capacities of connections having multiple bolts**

#### 4.2.2 Leading Edge Distance, $L_c$

By comparing the transition of failure modes as  $L_c$  is increased from 50.8 mm (2.0 in.) (BB) to 102 mm (4.0 in.) (BC) and finally to 152 mm (6.0 in.) (BD) an understanding and approximation of the of the bolt limit states may be made as shown in Table 11. The longitudinal shear capacity of the strips resisting the Type IV shear out failure falls between 6 – 10 MPa (0.87 – 1.45 ksi); this agrees well with the experimentally determined value of 6.7 MPa (Table 3). The bearing capacity corresponding to a Type I failure is essentially equal to the longitudinal capacity of the material reported in Table 2. The bearing associated with Type II splitting failure is also very close to, although lower than this latter value based on the hierarchy of failures observed. The observed progression of failure modes is shown in Figure 15.

**Table 11 – Summary of the effect of leading edge distance and associated single bolt failure modes**

geometry	$L_c$	$P_u$	failure mode	stress resulting from $P_u$	
				shear out (IV)	bearing force (VI)
				$P_u/(2L_ct)$	$P_u/ht$
				MPa	MPa
BB	50.8	6.92	IV	10.6	85.1
BC	102	7.83	II, IV	6.0	96.3
BD	152	8.67	II, VI	4.6	106.7

Longitudinal shear capacity was observed to fall between 6-10 MPa



$L_c = 50.8 \text{ mm}$   
 $\tau_{shear \text{ out}} = 10.6 \text{ MPa}$   
 $\sigma_{bearing} = 85.1 \text{ MPa}$

a) shear out

Bearing strength to cause splitting is slightly lower than  $F_{uL}$



$L_c = 102 \text{ mm}$   
 $\tau_{shear \text{ out}} = 6.0 \text{ MPa}$   
 $\sigma_{bearing} = 96.3 \text{ MPa}$

b) shear out and splitting

Bearing (plowing) capacity is similar to longitudinal capacity of material,  $F_{uL}$



$L_c = 152 \text{ mm}$   
 $\tau_{shear \text{ out}} = 4.6 \text{ MPa}$   
 $\sigma_{bearing} = 106.7 \text{ MPa}$

c) splitting and bearing

**Figure 15 - Failure mode transitions**

### 4.2.3 Longitudinal Bolt Spacing, $s$

Bolts aligned in the same longitudinal gage ‘shadow’ each other. The leading bolt carries more load, shadowing the trailing bolts. For this reason a minimum bolt spacing is conventionally prescribed [e.g., AISC 2010]. In comparing the results of all specimens having  $N = 2$  bolts, it is seen that BE, having  $s = 50.8$  mm (2.0 in.), has a lower capacity than the other specimens having  $s \geq 102$  mm (4.0 in.). This is an indication that the spacing,  $s$ , required to ensure that the capacity of all bolts along a gage line are engaged is approximately 102 mm (4.0 in.), or 8 bolt diameters, since the capacity does not appear to increase for  $s > 102$  mm (4.0 in.).

**Table 12 – Capacities of specimens having  $N = 2$**

	BE	BF	BG	BH	SC	SD
$s$ (mm)	50.8	102	102	152	-	-
$P_u$ (kN)	10.7	13.5	15.8	14.1	14.1	13.8

### 4.2.4 Bolt Diameter

Only three geometries were tested with 12.7 mm (0.5 in.) bolts and 25.4 mm (1.0 in.) bolt sleeves. There was no significant difference in the capacities or failure modes of single bolt connections (BB and BC) although a single BC specimen exhibited a Type VII pull-through failure which may have resulted from the bolt not being sufficiently tightened. For two bolts in a single gage line (geometry BE), the larger bolt sleeve resulted in a transition from a splitting (Type II) to a shear out (Type IV) failure and a marginally greater capacity. The wider bearing

area is believed to have reduced the concentrated stress that initiates the splitting (II) failure although more study of this effect is necessary.

#### **4.2.5 Effect of Stagger**

Similar to the open-hole tests, although more pronounced, the effect of staggering the bolts was to increase the capacity of the connection relative to a single row of bolts (see Table 9). For geometries in which the staggered holes are relatively close, a complex ‘block shear’ (Type V) failure was observed. This failure is a combination of longitudinal splitting and shear or tension rupture (See Figure 13). In a staggered connection, a longitudinal splitting failure will initiate an unbalanced force across a section due to the loss of connection symmetry; this leads to the subsequent shear or tension rupture portion of the failure.

### **4.3 SUMMARY**

Bolted lap-splice tests identified a number of limit states and provided initial guidance for designing bolted connections of the engineering bamboo strip material considered. In no case was the bolted connection tested able to reach the net section rupture capacity of the bamboo strip indicating that this limit state is unlikely to be critical in the envisioned connections.

Connections having multiple bolts exhibited a marginally reduced proportional capacity. For connections with fewer than five bolts, only about 85% of the sum of the single bolt capacities could be achieved.

Figure 16 summarizes the observed limitations for the strip material. A leading edge distance,  $L_c$ , of 152 mm (6.0 in.), corresponding to 12 bolt diameters, is necessary to develop the bearing capacity of the bolted connection against the bamboo. Additionally, the longitudinal shear-out capacity of the strip was determined to fall between 6 and 10 MPa (0.87 – 1.45 ksi), requiring  $L_c > 102$  mm (4.0 in.) (8 bolt diameters) to mitigate this failure. For values of  $L_c$  between 8 and 12 bolt diameters, a splitting failure was observed. Similarly, for bolts in the same gage line, longitudinal spacing,  $s$  exceeding 102 mm (4.0 in.) (8 bolt diameters) is required to ensure that the capacity of the adjacent bolts is obtained.

The results of this pilot study indicate that engineered bamboo strip material may represent a viable alternative for tensile-driven repairs of timber structures. The strips themselves exhibited material properties similar to those of timber while the bolted connections demonstrate predictable limits states behaviour.

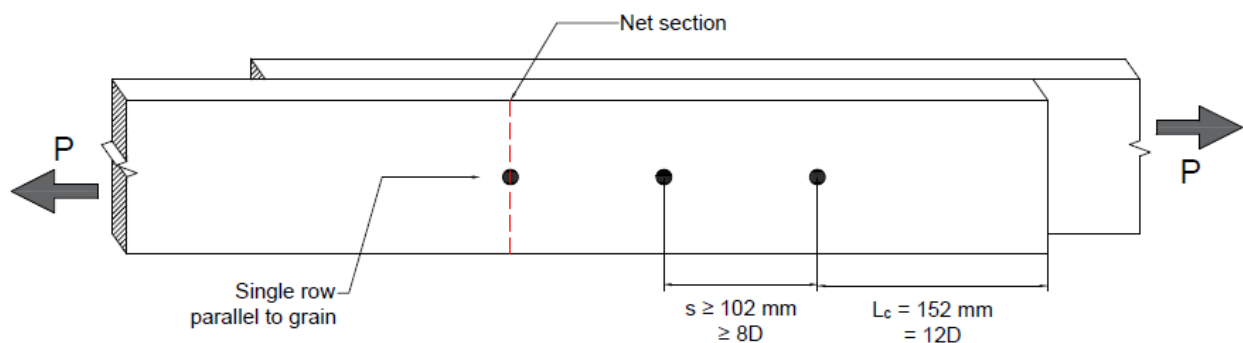


**Figure 16 – Minimum leading edge and spacing criteria (12.7 mm diameter bolts)**

## **5.0 FLEXURAL REPAIR OF TIMBER USING BAMBOO STRIPS**

### **5.1 INTRODUCTION**

When it comes to the repair or need for retrofitting of *in-situ* wooden dimensional lumber or timbers; one may ask, why not use steel as the repair or retrofit medium? Although this is often done, one problem resides in the variation in the materials' stiffness. The stiffness of materials as measured by their modulus of elasticity (MOE) should be compatible so as to not disrupt the structure's intended behavior. If a material with a stiffer or higher MOE is introduced into an existing system, the stiffer member or repair will preferentially attract the load and may induce a failure at the interface of the stiff repair and more flexible substrate. In this respect, steel has an MOE of approximately 200 GPa (29,000 ksi) while Douglas Fir timber, a common material used in timber bridges, has an MOE of only 11 GPa (1,600 ksi) (Kretschman 2012).

The engineered bamboo strip material used has an MOE on the order of 10 GPa (1,500 ksi) (Table 2) while exhibiting greater tensile strength than many wood species reported in the National Design Specification (NDS 1997). This, therefore, is the bases for the proposed repair and retrofit scheme.

## 5.2 FLEXURAL TEST PROGRAM

The NDS manuals provide two methods for determining design member capacities. One is through calculations using tabulated design values and a series of calculations, the other is through the use of pre-calculated ‘allowable’ design values which are based on a particular set of conditions and may be considerably less than those calculated manually. The allowable design values are calculated by adjusting the design values to accommodate particular conditions of the design. This is based on geometric constraints as well as service conditions including temperature and moisture among others (equation 5.4 and 5.5). The design values represent the 95% confidence interval determined from test results. The allowable design values are then used to select a member.

$$F'_b = F_b C_D C_M C_t C_L C_F C_{fu} C_r C_f \quad (5.4)$$

$$M' = F'_b \times S \quad (5.5)$$

Equations 5.4 and 5.5 (NDS 2015) represent the calculations of the allowable modulus of rupture (MOR),  $F'_b$ .  $F_b$  is the specified MOR for the timber species considered and each of the C factors accounts for an *in situ* stress condition, environment, or so forth (these are listed in the Nomenclature section of this thesis). The allowable design moment,  $M'$  is then found using the member elastic section modulus,  $S$ .

This flexural test program presented here is based on achieving the allowable modulus of rupture requirements of NDS. The test method is based on the method of ASTM D198.



### 5.2.1 Notched Timber

Notches in bending members should generally be avoided. This is particularly important on the tension face of the member. The increased stress concentrations at the corners of the notches may initiate both flexural cracks and longitudinal shear cracks; lumber, typically, has relatively low resistance to the latter. Notches located in the outer thirds of a flexural span having depths less than or equal to  $1/6^{\text{th}}$  the beam depth and lengths less than or equal to  $1/3^{\text{rd}}$  the beam depth have little effect on the beams stiffness (NDS 1997). There are no notches permitted at the tension face of sawn lumber with nominal thickness exceeding 102 mm (4 in.), except where the member is notched at its end for bearing over a support and those shall not be greater than  $1/4^{\text{th}}$  the beam depth as seen in Figure 17 (NDS 1997). In this study, notches will be provided in the middle third of 152 mm deep members. Such notches may arise from damage, re-use of members, change in support conditions (removal of support), construction error or intentionally, to accommodate a change in the structure. Typically, such members would require replacement or repair if found in situ.

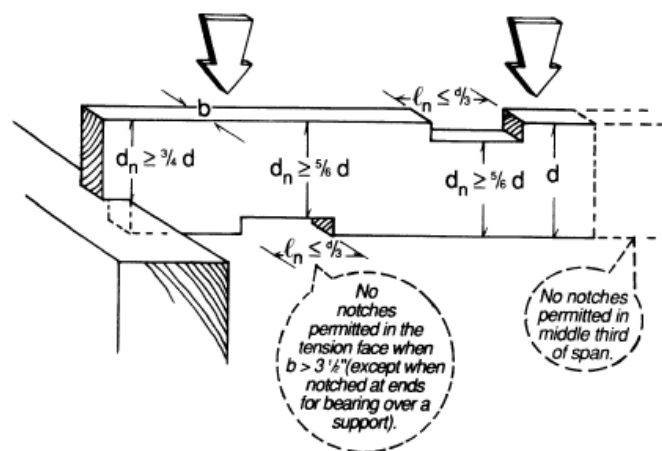
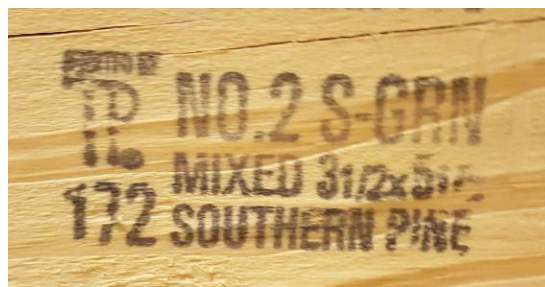


Figure 17 – Notch limitations for Sawn Lumber Beams (NDS 1997)

### 5.2.2 Test Specimens

The flexural test specimens used in this study are 140 x 90 mm (nominal 6 x 4 lumber) Southern Pine lumber. The grading stamp on the timber (Figure 18) indicates the material to be “No. 2 Grade Mixed Southern Pine” (as graded by Timber Products Inspection Company (TP)). The material was milled by Stanley Land and Lumber in Drake’s Branch VA (Mill number 172).



**Figure 18 – Lumber grading**

Such material is typically used in construction configurations such as joists, truss chords, or other similar members and placed in flexure about their strong axis. When calculating theoretical capacity, it was assumed that the tested members will represent members used in situations in which the moisture content will not exceed 19% for an extended period. The NDS provides tabulated values for pressure treated wood products of this dimensions and species. While the materials used are not pressure treated, the only differences between untreated and pressure treated timber are associated with the load duration factors which are not a consideration in this pilot test program.

Geometric measurements as well as any visual characteristics such as knots and checking were recorded. There was large variation in the test specimens – this is to be expected from No. 2

lumber. In particular, the amount and location of heartwood through the specimen section varied. Figure 18 shows the end grain of some of the tested members. The presence of heartwood was recorded along with its generalized location in the section.

Moisture content of the timber (following extended storage in a laboratory environment) at the time of testing was found to range between 12 and 16%

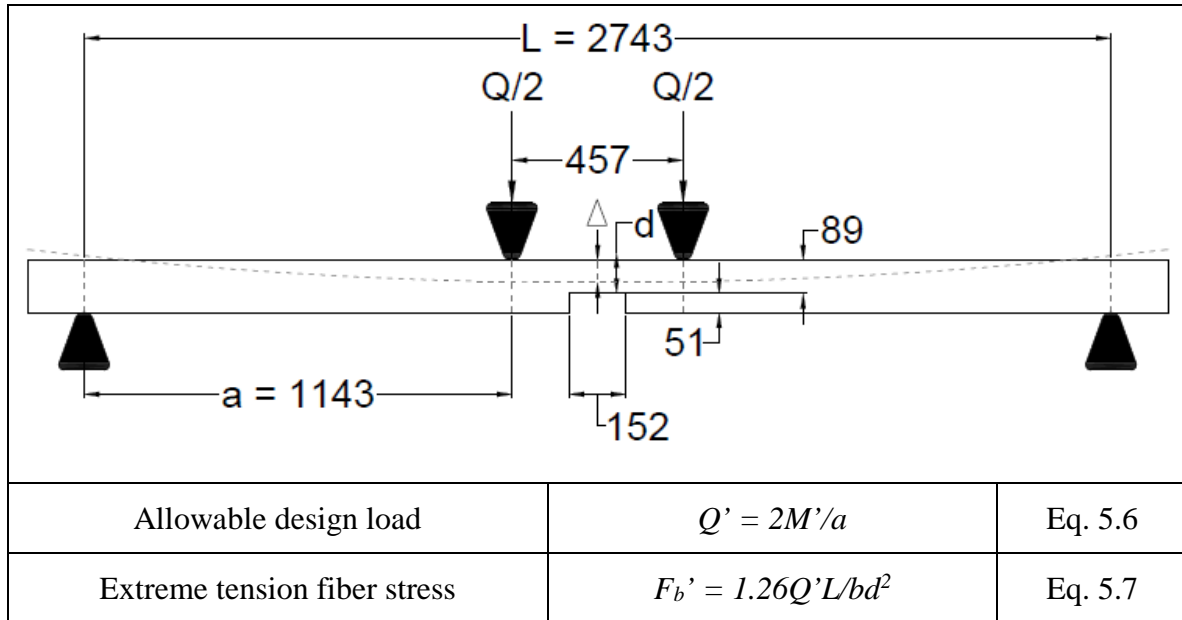


**Figure 19 – End grain view showing variation in heartwood inclusion.**

### **5.2.3 Test Arrangement**

Beams were tested in four-point flexure over span,  $L = 2743$  mm (108 in.). A 457 mm constant moment region was provided resulting in equal shear spans of  $a = 1143$  mm, (see Table 13). The beam specimens generally satisfied the requirements of ASTM D198, that is, they are longer than eight times their maximum section depth. Additionally, having a sectional dimension ratio of less than two, the beams require no lateral support beyond that provided inherently at the supports and loading locations.

Table 13 – Flexural beam test arrangement



The allowable moment,  $M'$ , is determined using equations 5.4 and 5.5, this is applied to equation 5.6 and the allowable design load is determined and will be compared with the achieved loads. The achieved extreme fiber stress and apparent modulus of elasticity are obtained using equations 5.7 and 5.8, respectively.

Using a 900 kN capacity servo-hydraulic universal testing machine equipped with a reaction frame for beam bending specimens having a length up to 3 m (10 ft), specimens were loaded in displacement control such that the maximum load was reached in not less than four minutes. The initial crosshead speed chosen rate was 1.27 mm / min. (0.05 in. /min.). Midpoint deflection of the beam was measured relative to the top surface of the beam using a Linear Position Transducer (String Potentiometer). Strain gages were installed centered on the laminated bamboo repair plate as well as centered in the notch of the beam (both described

below) in order to establish a comparison of attained strain capacity when compared with the open-hole and bolted lap-splice tests described in Chapters 3 and 4.

Data collected describes first failure, maximum load, and any points of sudden change. All recorded failures indicate their type, manner, order of appearance, and locations. The moisture content at a point near the failure zone but away from the ends of the beam was determined as per ASTM D7438-13.

Two beams with notches were tested in order to determine their reduced capacities; these were labelled CNa and CNb (control, notched). The tension face notches, located at the beam midspan, were approximately  $1/3^{\text{rd}}$  the beam depth resulting in a residual depth above the notch (Table 13)  $d = 89 \text{ mm}$  (3.5 in.) and had a length equal to the nominal depth (152 mm) (6.0 in.) of the beam. The loading points for all notched beam tests were located 152 mm (6.0 in.) from either edge of the notch. The notch was created using a router with a 25.4 mm (1 in.) bit. These beams were tested to failure.

A second series of four beams having the same notched design were repaired with bolted bamboo strips prior to testing (described below); these were labelled BN (bamboo, notched). This simulated a scenario of locating a defect in the field prior to loading.

Two un-notched control beams (Ca and Cb) were also tested to establish the member capacity.

Based on preliminary calculations using the NDS (1997), the allowable maximum moment for a 140 mm x 89 mm x 2743 mm (6 in. x 4 in. x 9 ft.) Southern Pine beam is 3.0 kN-m (26.5 kip-in) and the allowable tensile fiber stress is 8.5 MPa (1231 psi). These values are calculated using Table 4B from the NDS (1997) and the equations listed in Table 13. If that beam is “damaged” resulting in a loss of cross sectional area equal to  $1/3^{\text{rd}}$  of the beam’s original

area, the allowable moment would decrease to 1.3 kN-m (11.8 kip-in.) and the allowable tensile fiber stress increases slightly to 9.2 MPa (1340 psi) as shown in Table 14.

The proposed repair involves bolting a strip of the engineered bamboo across the notch. The bamboo strip will help to distribute the tension stresses around the notch by providing an alternate load path across the notch. The strip should also reduce some of the stress raising effect of the notch by relieving the stresses at the reentrant corners at the top of the notch. Based on conventional timber preservation practice (United States Department of the Interior 1995), the strips are bolted to the substrate timbers. Bolt pattern is a parameter considered in this pilot study.

The bamboo strip was cut to have a width equal to beam soffit ( $b = 89$  mm). The bamboo strip was clamped to each beam. The bolt pattern was then transferred to the clamped set up and drilled in two steps providing a counter bore for the unthreaded portion of the lag screw. The lag screws were “snug” tightened against 35 mm (1.4 in.) washers so as to not crimp or bear into the bamboo fibers. The longitudinal edge distance,  $L_c = 8D = 102$  mm was provided in every case. This value is sufficiently large to mitigate a shear-out failure (see Section 4.2.2).

Bolting requirements follow NDS (1997) guidelines for the timber member. Capacity of the bamboo strips are based on the limit states investigated in Chapters 3 and 4. Design values for the number of lag screws used is based on the withdrawal values for penetration depths less than the full value of  $8D$  but greater than  $4D$  therefore requiring a reduction in capacity ( $D$  is the nominal bolt diameter). A 63.5 mm (2.5 in.) lag screw having a diameter of 12.7 mm (0.5 in.) placed through 6.4 mm (0.25 in.) of bamboo will yield a withdrawal design value of 2.2 kN (494 lb.) per screw loaded laterally in Southern Pine. This value is less than the single bolted lap

splice capacities determined in Chapter 4 and is therefore the critical limit state for a single bolt (Table 14).

**Table 14 – Single Bolt Shear Capacity Limit States**

limit state	nominal capacity	characteristic capacity <sup>a</sup>	source
12.7 mm lag screw embedded approximately 4.5D in Southern Pine	-	2.2 kN	NDS 1997
12.7 mm bolt in 12.7 mm hole in bamboo strip with $L_c = 102$ mm	7.8 kN	6.4 kN	geometry BC
bolt bearing in bamboo strip = $D \times t \times F_u$	7.5 kN	4.8 kN	Tables 11 and 2
<sup>a</sup> mean minus three standard deviations			

The bolting geometries considered consisted of 6 lag screws (per side) and were chosen based on open-hole capacities, single inline gage bolted capacities, and multiple gage staggered bolt capacities as previously determined in Chapters 3 and 4. Two bolting arrangements were considered: Beams BNa and BNb (bamboo, notched) had two gage lines of three bolts each. The gage distance  $g = 3D = 38.1$  mm and longitudinal spacing,  $s = 5D = 63.5$  mm. Beams BNSa and BNSb had a staggered arrangement with three gage lines also having  $s = 5D = 63.5$  mm and a staggered gage  $g = 2D = 25.4$  mm. Bolt details are shown in Figure 17. Table 15 summarizes the relevant limit states. It is seen that the ‘design’ tension (based on the characteristic material properties defined as the mean minus three standard deviations) that may be carried by the bamboo strip is 13.2 kN based on the Southern Pine bolt withdraw capacity and slightly greater than this for the bolted connections through the bamboo strip (13.4 and 14.9 kN for BN and BNS, respectively). Thus the six bolt arrangements are adequate to achieve the critical limit state of the substrate timber.

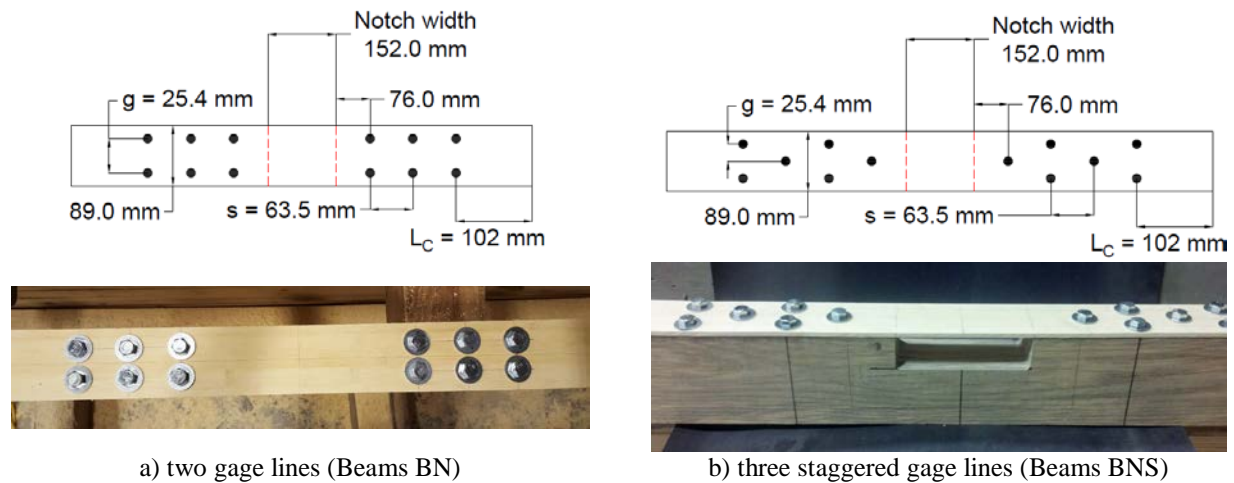


Figure 20 – Bolt details on notched beams

Table 15 –Bamboo Strip Tension Capacity Limit States

bamboo strip limit state	nominal capacity	characteristic capacity <sup>a</sup>	failure type expected (Figs 9 and 13)	geometry or calculation (Chapters 2 – 4)
tensile stress capacity	91.8 MPa	58.8 MPa	I	Batch 2 (Table 2)
gross section capacity	52.3 kN	33.5 kN		
6 x single bolt capacity (timber)	-	13.2 kN	timber	Table 14
0.85 x 6 x single bolt capacity (bamboo)	35.3 kN	22.4 kN	IV	Table 14 and Eq. 4.2
<b>two gage lines (BN)</b>				
net section capacity, $g = 38.1$ mm	33.6 kN	21.5 kN	I	Eq. 3.1; $k = 0.9$
single row of bolts, $g = 38.1$ mm, $L_c = 102$ mm	13.8 kN	13.4 kN	II, IV or V	SD
shear out with $L_c = 102$ mm	15.7 kN	<sup>b</sup>	IV	Table 11 with shear capacity = 6 MPa
<b>three staggered gage lines (BNS)</b>				
net section capacity, $g = 25.4$ mm	26.9 kN	17.2 kN	I	Eq. 3.1; $k = 0.9$ ; no effect of stagger
single stagger line, $g = 25.4$ mm, $s = 63.5$ mm, $L_c = 102$ mm	21.3 kN	14.9 kN	II	SJ
shear out with $L_c = 102$ mm and 165 mm	33.3 kN	<sup>b</sup>	IV	Table 11 with shear capacity = 6 MPa
<sup>a</sup> mean minus three standard deviations				
<sup>b</sup> insufficient data to prescribe characteristic value of shear capacity				



### 5.3 FLEXURAL TEST RESULTS AND DISCUSSION

A summary of test results are provided in Table 16.

**Table 16 Summary of beam test results**

	depth, $d$	$Q_{max}$	$M_{max}$	$F_b'$ at $d$	$\Delta_{max}$	$\varepsilon_{b,max}$	$P_{max}$
	mm	kN	kNm	MPa	mm	$\mu\varepsilon$	kN
		$Q = 2M/a$	$M = Qa/2$	$F_b' = 6M/bd^2$			$P = E_b \varepsilon_b w t$
<b>allowable design values</b>							
full section	140	3.34	2.29	7.93	-	-	-
1/3rd notch	98	1.53	1.05	8.96	-	-	-
<b>test specimens</b>							
Ca	139	29.3	16.7	58.4	129.7	-	-
Cb	139	26.2	15.0	52.2	48.0	-	-
CNa	88.4	9.6	5.5	47.3	73.3	-	-
CNb	88.3	5.9	3.4	29.2	43.2	-	-
BNa	87.5	10.1	5.8	50.8	54.0	4471	26.0
BNb	87.1	10.4	5.9	52.8	53.4	5100	27.8
BNSa	88.4	7.6	4.3	37.5	40.2	4322	23.5
BNSb	87.7	10.6	6.1	53.1	35.4	5006	27.2
$Q_{max}$ maximum total load applied to beam over both load points $M_{max}$ moment corresponding to $Q_{max}$ $F_b'$ MOR at extreme tension face of timber (bottom of d) $\Delta_{max}$ maximum midspan deflection $\varepsilon_{b,max}$ maximum strain recorded in bamboo strip $P_{max}$ maximum tension in bamboo strip; $E_b$ is taken as 9640 MPa (Table 2)							

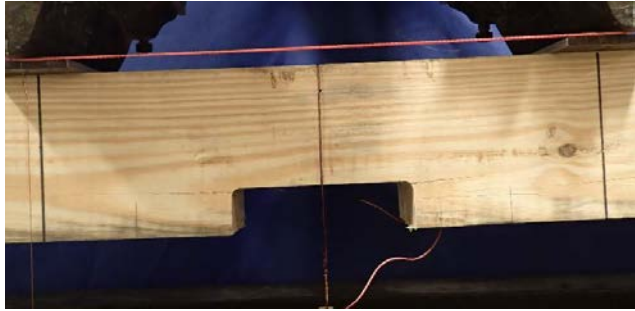
In general, experimental capacities exceeded NDS ‘allowable’ capacities by a significant degree indicating a considerable inherent ‘factor of safety’ in the design approach.

The presence of the notches affected a significant reduction in capacity over the full section beam. The degree of reduction was greater than allowable design values would suggest. The addition of bolted bamboo strips affected a modest improvement in load carrying capacity

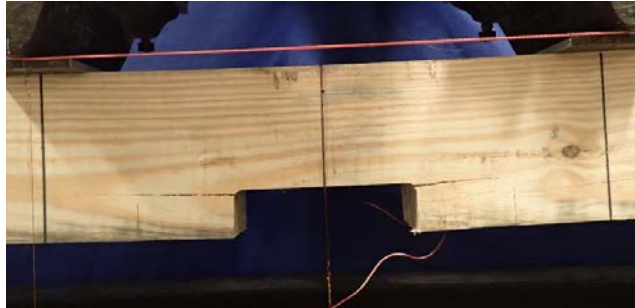
and a marked improvement in the ability of the notched section to efficiently utilize its modulus of rupture capacity. In the full section Beams C,  $F_b'$  was greater than 50 MPa ( $F_b'$  is expected to exhibit considerable variation). In the notched Beams CN,  $F_b'$  is observed to fall well below 50 MPa. The addition of the bolted bamboo strips results in some of this loss being recovered in Beams BN and BNS. This behavior is discussed in Section 5.4, below.

Failure modes were predominately initiated at the radius of the notches due to the stress concentration at this location. Figures 21a and 22a show the longitudinal crack in notched specimens CNa and CNb, respectively, just after initiation; propagation and eventual longitudinal shear failure along the grain are shown in corresponding figures b and c, respectively. Throughout crack growth, load carrying capacity remains near constant as deflection continues.

The inclusion of knots is always a concern and it is difficult to determine their effect on member capacity. Their location and depth relative to the notch may have a detrimental effect. This is seen in both Figures 21c and 22c as the final failure plane is influenced by the presence of knots. Other beams displayed behavior that appeared to be unaffected by a specific defect.



a) initiation of longitudinal crack at notch root

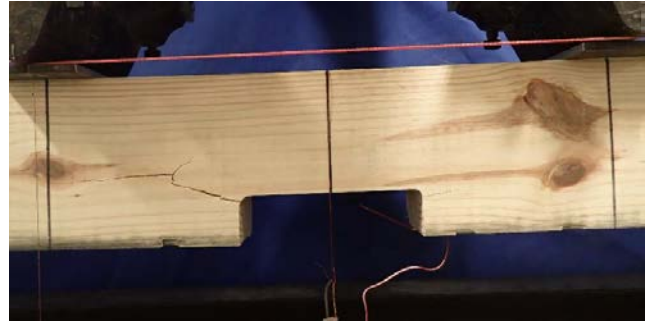


b) propagation of crack

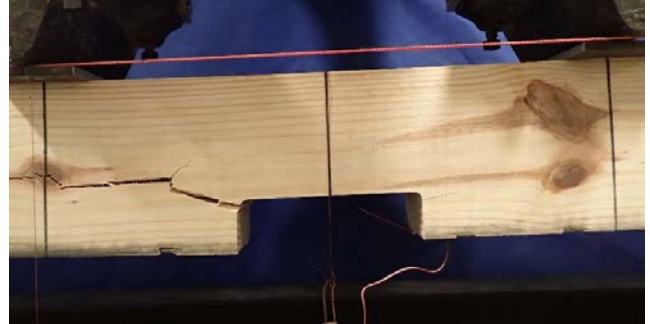


c) longitudinal shear along the grain failure  
note knot to right of notch affecting final failure

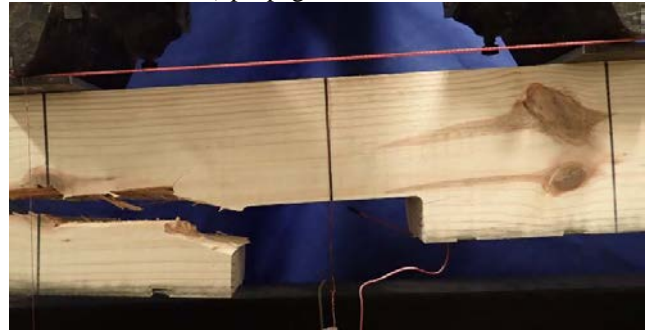
**Figure 21 – Failure progression of Beam CNa**



a) initiation of longitudinal crack at notch root



b) propagation of crack



c) longitudinal shear along the grain failure  
note significant knot to left of notch affecting final failure

**Figure 22 – Failure progression of Beam CNb**

Beam BNSa had a color variation (Figure 22) perhaps indicating previous water damage or biological attack. Although virtually free of knots, checks, or any other distinguishing marks other than its greyish color, this beam exhibited a markedly reduced capacity by comparison to the other repaired beams (Table 16).

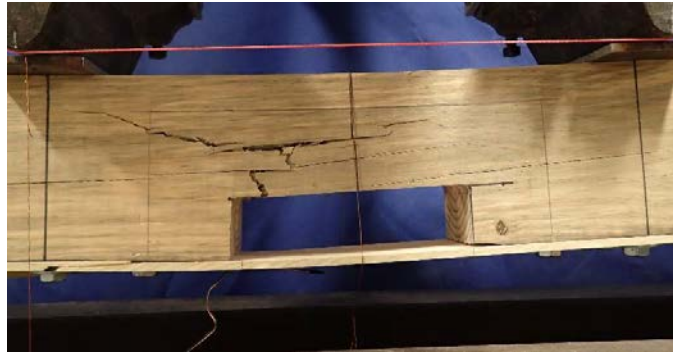


**Figure 23 – Beam with color variation (Beam BNSa)**

Following the initiation of the crack, all repaired beams maintained their capacity while the bamboo allowed for deflections to increase (Figure 24). The bolted bamboo repairs eventually failed exhibiting Type V failure modes (see Figure 13) similar to those seen in the bolted lap tests as seen in Figure 25.

The resulting tension force carried by the bamboo strips is given in Table 16 calculated based on strains recorded at the strip gross section. These forces all exceed the characteristic design capacity reported in Table 15 by a factor of approximately two. Failure Type V is a somewhat mixed mode of response in which case comparison with nominal predicted capacities is difficult. Nonetheless, the strips developed tensile forces similar to those seen in the bolted lap splice tests reported in Chapter 4.



**Figure 24 – Beam at failure of bamboo (Beam BNa)**



a) Type V failure of two gage line bolt pattern (Beam BNa)



b) Type V failure of staggered three gage line bolt pattern (Beam BNSa)

**Figure 25 – Failures of bolted bamboo strips**

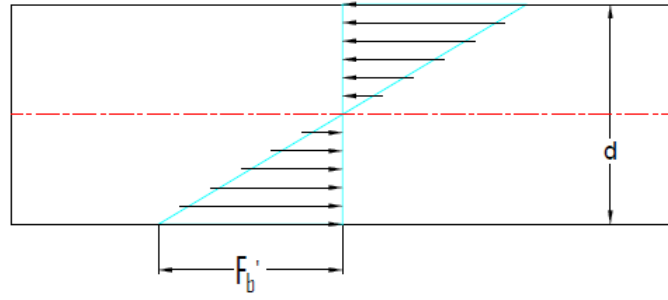
## **5.4 SUMMARY**

Flexural tests on un-altered Southern Yellow Pine specimens displayed properties well above those prescribed by the NDS allowable strength design approach. The apparent ‘factors of safety’ are on the order of 3 to 7 in the present study. While the addition of the laminated bamboo strip material to the notched specimens allowed for minimal increase in load carrying

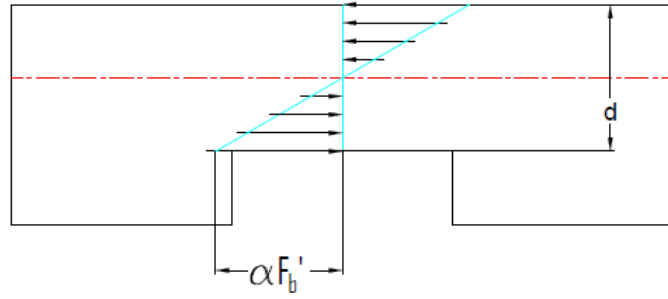
capacity, the tested arrangements only restored on the order of 20% of the notched member capacity.

The mechanism by which the bamboo strip tension reinforcement affects capacity is illustrated in Figure 26 and described as follows:

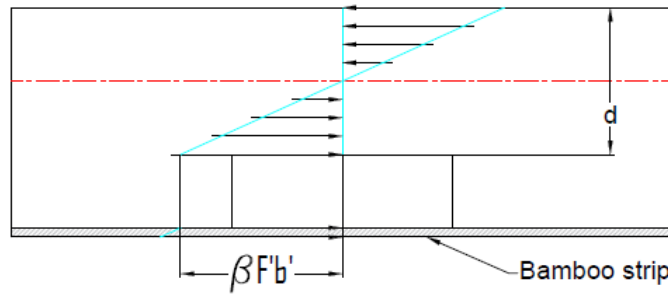
1. The flexural capacity of the un-notched beam (Figure 26a) in flexure is governed by the modulus of rupture  $F_b'$ . The moment capacity is given by Eq. 5.5.
2. The flexural capacity of the notched beam (Figure 26b) is clearly reduced due to the reduction in section modulus,  $S$ , however the apparent modulus of rupture is also reduced:  $\alpha F_b'$ , where  $\alpha < 1.0$ . This reduction reflects the stress raising effects of the notch itself. The notch is less tough than the un-notched timber and therefore cracking initiates earlier, typically at the root of the notch as clearly seen in Figures 21 and 22. In this study, the notch was provided with a 12.7 mm radius at its root, resulting in an apparent value of  $\alpha \approx 0.69$  (comparing Beams CN to C). A smaller radius or saw cut notch would be expected to result in a lower value of  $\alpha$ .
3. By bridging the notch with the bamboo strip (Figure 26c), an alternate load path for the tension stress is provided. This relieves some of the tension stress that must cross the root of the notch. While the stress raising effect of the notch remains the same, the stress is reduced and the apparent modulus of rupture is partially restored:  $\beta F_b'$ , where  $\alpha < \beta < 1.0$ . In this study,  $\beta \approx 0.88$ .



a)  $F_b'$



b)  $\alpha F_b'$  ( $\alpha \approx 0.69$ )



c)  $\beta F_b'$  ( $\beta \approx 0.88$ )

**Figure 26 – Stress distribution**

## **6.0 CONCLUSIONS AND RECOMENDATIONS FOR FUTURE WORK**

Using a limit states approach, it is necessary to address all manners by which a structure or element may fail and design for these. The focus of the current work is bolted connections for engineered bamboo-strip repairs of timber members. The limit states of the connection include bolt shear; bearing/splitting of bamboo; shear-out of bamboo, and net section failure of bamboo. In the present work steel bolts are considered, in which case bolt shear is not a controlling limit state.

This study incorporated three batches of engineered bamboo strip from the same source. These included both natural and caramelized variations. Some variation of material properties was seen between these and a significant loss of lignin-dominated transverse properties was observed for the caramelised version of the material. As a result the bolted applications were limited to the use of the natural strip material.

A method for determining longitudinal shear capacity and modulus based on ASTM D3846 was demonstrated. Specimens that were too thin and larger notch kerfs introduced some Mode I behaviour along the shear plane requiring adjustment to the prescribed test geometry of ASTM D3846. Combinations of 50 mm wide specimens having 1 mm kerf notches appeared to mitigate this issue.



Open-hole tests of engineered bamboo strips displayed reliable patterns of material behaviour. Net section reduction factors accounting for the stress-raising effect of the holes were identified to be a function of hole diameter and material anisotropy (Table 5). While no net section reduction was observed for 12.7 mm (0.5 in.) holes in 89 mm (3.5 in.) wide specimens, a reduction factor of 0.8 was observed for 25.4 mm (1.0 in.) holes in the same material. A reduction of 0.9 was observed for 12.7 mm (0.5 in.) holes in a caramelised material ( $F_{uL}/F_{uT} = 22.8$ ) in which the transverse material properties are proportionally lower than in the natural material ( $F_{uL}/F_{uT} = 14.0$ ) resulting in much greater degree of anisotropy (Table 2).

DIC testing illustrates that as the degree of anisotropy varies, the ability of the material to effectively ‘channel’ stress (as illustrated by strains) around holes is affected. With increasing anisotropy, the behaviour transitions from one of 45° shear-dominated stresses leading to a transverse crack emanating from the hole – a classic net section failure observed in steel – to a behaviour characterised by longitudinal shear stresses. This behaviour will affect bolted connection design of bamboo strips in at least the following ways:

1. The shear-out limit state will likely dominate over net section behaviour.
2. The beneficial effects of staggering bolt holes in orthotropic materials will likely not be realised.
3. Multiple bolts along the same gage line may become proportionally less effective.

All of these effects were observed to some extent in the present study as indicated below.

Bolted lap-splice tests identified a number of limit states and provided initial guidance for designing bolted connections of the engineering bamboo strip material considered. In no case was the bolted connection tested able to reach the net section rupture capacity of the bamboo strip indicating that this limit state is unlikely to be critical in the envisioned connections.

The impact of staggering the holes was observed to depend on the spacing between holes. Additional study is necessary to quantify these effects since the effect of introducing the hole is detrimental (Table 5), while the effect of staggering the holes may counteract this effect to a small degree (Table 6).

A leading edge distance,  $L_e$ , of 152 mm (6.0 in.), corresponding to 12 bolt diameters, is necessary to develop the bearing capacity of the bolted connection against the bamboo. Similarly, for bolts in the same gage line, longitudinal spacing,  $s$  exceeding 102 mm (4.0 in.) (8 bolt diameters) is required to ensure that the capacity of the adjacent bolts is obtained.

Flexural tests on the selected un-altered Southern Yellow Pine specimens displayed properties well above those prescribed by the NDS guide. An inherent ‘over strength factor’ of approximately 7 was observed. While the addition of the laminated bamboo strip material to the notched specimens allowed for a marginal minimal increase in capacity, the tested arrangements did not restore an appreciable amount of the original capacity. The tests did clearly illustrate, however, that the limit states described in chapters 2 through 4 were achievable and a relatively reliable indication of performance. This suggests that utilizing the limit state based design approach, a practical method of utilizing and/or optimizing the engineered bamboo strip material may be accomplished.


The results of this pilot study indicate that engineered bamboo strip material may represent a viable alternative for tensile-driven repairs of timber structures. The strips themselves exhibited material properties similar to those of timber while the bolted connections demonstrate predictable limits states behaviour. The highly anisotropic nature of the strips limited their performance suggesting the laminated veneer bamboo may provide a better alternative for the envisioned applications.

## APPENDIX A

### TEST RESULTS


#### A.1 ENGINEERED BAMBOO STRIP MATERIAL PROPERTIES

Geometry	A		
Batch	1	Natural	
No. holes	N	0	-
Diameter of holes	h	-	in
Hole gage	g	-	in
Hole spacing	s	-	in
Leading edge	L <sub>c</sub>	-	in
Modulus	E <sub>L</sub>	1475894	psi
Strength	F <sub>u</sub>	13768	psi
Capacity	P <sub>u</sub>	11893	lbf




Geometry	Width	Thickness	Max Load	Max Stress	Max Strain
A	(in)	(in)	(lbf)	(psi)	(in/in)
1	3.53	0.24	10196	11840	8185
2	3.53	0.25	13546	15616	10798
3	3.53	0.25	10694	12279	9009
4	3.52	0.25	12009	13829	11570
5	3.53	0.24	11968	13876	8215
6	3.54	0.24	10685	12454	-
7	3.53	0.24	13015	15153	-
8	3.54	0.24	13034	15100	-
Mean	3.53	0.24	11893	13768	9555
COV	0.00	0.01	0.11	0.11	0.16

Geometry	A		
Batch	1	Caramelized	
No. of holes	N	0	-
Diameter of holes	h	-	in
Hole gage	g	-	in
Hole spacing	s	-	in
Leading edge	L <sub>c</sub>	-	in
Modulus	E <sub>L</sub>	1268488	psi
Strength	F <sub>u</sub>	13416	psi
Capacity	P <sub>u</sub>	11628	lbf




Geometry	Width	Thickness	Max Load	Max Stress	Max Strain
A	(in)	(in)	(lbf)	(psi)	(in/in)
1	3.54	0.24	9937	11708	7881
2	3.53	0.26	11262	12314	10885
3	3.50	0.26	14087	15533	13323
4	3.47	0.24	12295	14803	8932
5	3.47	0.24	10559	12724	8510
Mean	3.50	0.25	11628	13416	9906
COV	0.01	0.04	0.14	0.12	0.22

Geometry	A (Transverse)		
Batch	1	Natural	
No. of holes	N	0	-
Diameter of holes	h	-	in
Hole gage	g	-	in
Hole spacing	s	-	in
Leading edge	L <sub>c</sub>	-	in
Modulus	E <sub>T</sub>	126750	psi
Strength	F <sub>u</sub>	985	psi
Capacity	P <sub>u</sub>	385	lbf




Geometry	Width	Thickness	Max Load	Max Stress	Max Strain
A <sub>Transverse</sub>	(in)	(in)	(lbf)	(psi)	(in/in)
1	1.37	0.24	62	185	1604
2	1.62	0.24	349	885	7443
3	1.75	0.24	366	876	11901
4	1.76	0.24	412	967	5709
5	1.33	0.24	354	1112	7675
6	1.67	0.25	445	1084	8116
7	3.37	0.24	893	1085	5048
8	3.27	0.25	1064	1327	6456
Mean	1.62	0.24	385	985	8169
COV	0.11	0.01	0.11	0.11	0.28

Geometry	A (Transverse)		
Batch	1	Caramelized	
No. of holes	N	0	-
Diameter of holes	h	-	in
Hole gage	g	-	in
Hole spacing	s	-	in
Leading edge	L <sub>c</sub>	-	in
Modulus	E <sub>L</sub>	1268488	psi
Strength	F <sub>u</sub>	13416	psi
Capacity	P <sub>u</sub>	11628	lbf




Geometry	Width	Thickness	Max Load	Max Stress	Max Strain
A <sub>Transverse</sub>	(in)	(in)	(lbf)	(psi)	(in/in)
1	3.50	0.23	840	1041	8402
2	2.88	0.23	451	680	4744
3	2.90	0.23	357	530	3632
4	2.93	0.23	438	642	3911
5	2.89	0.24	425	627	4283
6	2.91	0.24	571	827	8510
7	-	-	-	-	2917
8	2.92	0.24	322	466	2032
Mean	2.90	0.23	399	589	3720
COV	0.01	0.01	0.14	0.15	0.28

Geometry	A		
Batch	2	Natural	
No. of holes	N	0	-
Diameter of holes	h	0.00	in
Hole gage	g	0.00	in
Hole spacing	s	0.00	in
Leading edge	L <sub>c</sub>	0.00	in
Modulus	E <sub>L</sub>	1398269	psi
Strength	F <sub>u</sub>	13321	psi
Capacity	P <sub>u</sub>	11613	lbf



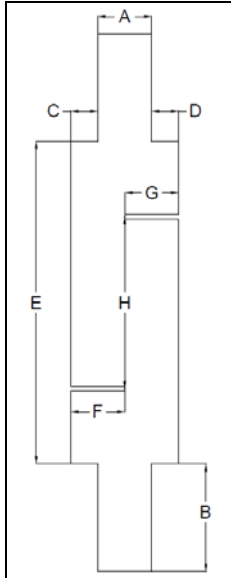
Geometry	Width	Thickness	Max Load	Max Stress	Max Strain
A	(in)	(in)	(lbf)	(psi)	(in/in)
1	3.54	0.25	10489	12041	-
2	3.53	0.25	12883	14813	-
3	3.54	0.25	11097	12672	-
4	3.53	0.25	10299	11762	-
5	3.51	0.25	13297	15314	-
Mean	3.53	0.25	11613	13321	-
COV	0.00	0.00	0.12	0.12	-

Geometry	A		
Batch	2	Natural (Transverse)	
No. of holes	N	0	-
Diameter of holes	h	0.00	in
Hole gage	g	0.00	in
Hole spacing	s	0.00	in
Leading edge	L <sub>c</sub>	0.00	in
Modulus	E <sub>L</sub>	203427	psi
Strength	F <sub>u</sub>	1136	psi
Capacity	P <sub>u</sub>	820	lbf

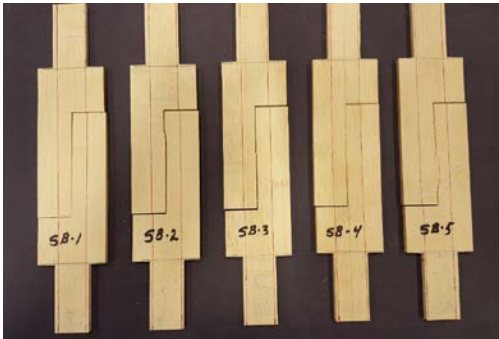


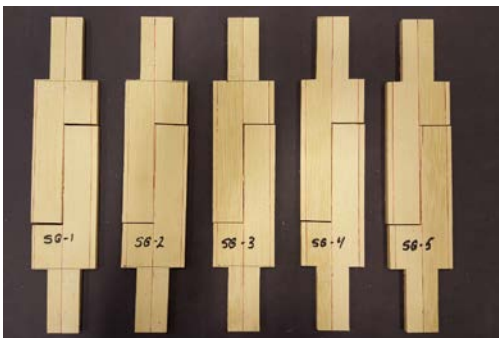
Geometry	Width	Thickness	Max Load	Max Stress	Max Strain
A	(in)	(in)	(lbf)	(psi)	(in/in)
1	3.07	0.25	700	1008	5032
2	3.07	0.25	800	1096	6808
3	3.07	0.25	900	1199	5755
4	3.09	0.24	200	371	689
5	3.08	0.25	900	1299	6556
6	3.09	0.24	800	1079	4943
Mean	3.07	0.25	820	1136	5819
COV	0.00	0.01	0.10	0.10	0.15

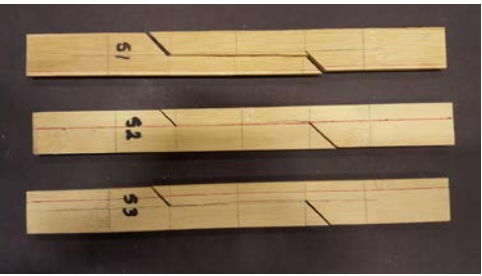
## A.2 SHEAR TEST

	A	Grip width
	B	Grip length
	C	Left shoulder
	D	Right shoulder
	E	Distance between grips
	F	Left notch length
	G	Right notch length
	H	Distance between notches
	T	Thickness of section between notches
	SB	Shear line in the bamboo culm section
	SG	Shear line along the glue line
	S	Shear section samples

Sample I.D.	A	B	C	D	E	F	G	H	T	A <sub>v</sub> (in <sup>2</sup> )	A+C+D
<b>SB-1</b>	1.00	1.98	0.46	0.51	5.92	0.97	0.97	3.11	0.25	0.77	1.97
<b>SB-2</b>	1.00	1.98	0.45	0.51	5.92	0.98	0.98	3.11	0.25	0.78	1.96
<b>SB-3</b>	1.00	1.97	0.47	0.50	5.94	0.99	0.98	3.13	0.25	0.77	1.97
<b>SB-4</b>	0.98	1.98	0.48	0.51	5.89	0.97	0.98	3.09	0.25	0.77	1.97
<b>SB-5</b>	1.00	1.97	0.47	0.50	5.91	0.99	0.97	3.09	0.25	0.76	1.97
<b>SG-1</b>	1.00	1.97	0.49	0.49	5.91	0.95	1.02	3.11	0.25	0.77	1.97
<b>SG-2</b>	1.00	1.97	0.48	0.49	5.94	0.99	1.02	3.14	0.25	0.78	1.97
<b>SG-3</b>	1.00	1.97	0.47	0.49	5.94	0.97	0.99	3.14	0.25	0.78	1.96
<b>SG-4</b>	1.00	1.97	0.47	0.50	5.90	0.96	0.99	3.11	0.25	0.77	1.97
<b>SG-5</b>	0.99	1.97	0.49	0.50	5.90	0.99	0.99	3.10	0.25	0.77	1.97
<b>S1</b>	0.96							3.19	0.25	0.79	
<b>S2</b>	0.99							3.15	0.25	0.78	
<b>S3</b>	1.00							3.19	0.25	0.79	
<b>Mean</b>	0.99							3.13	0.25	0.78	1.97
<b>COV</b>	0.02							0.01	0.01	0.01	0.00

Culm Section Mid Line (SB)				
Specimen	Max Load	Max Stress	Shear Modulus	
	(lbf)	(psi)	(ksi)	
SB-1	679	876	381771	
SB-2	767	983	445829	
SB-3	837	1089	347264	
SB-4	919	1187	370844	
SB-5	930	1221	475172	
Mean	826	1071	-	
COV	0.13	0.13	-	


Glue Line (SG)				
Specimen	Max Load	Max Stress	Shear Modulus	
	(lbf)	(psi)	(ksi)	
SG-1	749	968	422376	
SG-2	688	887	472719	
SG-3	728	937	492176	
SG-4	765	990	505868	
SG-5	812	1052	533071	
Mean	749	967	485242	
COV	0.06	0.06	0.09	

Mixed Mode Failures (S)				
Specimen	Max Load	Max Stress	Shear Modulus	
	(lbf)	(psi)	(ksi)	
S1	431	548	315895	
S2	480	614	364900	
S3	507	641	296370	
Mean	473	601	325722	
COV	0.08	0.08	0.11	




### A.3 OPEN-HOLE TENSION TEST

Geometry	OB		
Batch	1	Natural	
No. of holes	N	1	-
Diameter of holes	h	0.50	in
Hole gage	g	0.00	in
Hole spacing	s	0.00	in
Leading edge	L <sub>c</sub>	-	in




Geometry	Width	Thickness	Max Load	Max Stress	Max Strain
OB	(in)	(in)	(lbf)	(psi)	(in/in)
1	3.52	0.25	10488	14196	6432
2	3.52	0.24	8451	11437	5389
3	3.52	0.24	8227	11183	5409
4	3.52	0.25	9912	13323	6773
5	3.52	0.25	8893	11938	4849
Mean	3.52	0.25	9194	12415	5770
COV	0.00	0.01	0.11	0.10	0.14

Geometry	OB		
Batch	1	Caramelized	
No. of holes	N	1	-
Diameter of holes	h	0.50	in
Hole gage	g	0.00	in
Hole spacing	s	0.00	in
Leading edge	L <sub>c</sub>	-	in



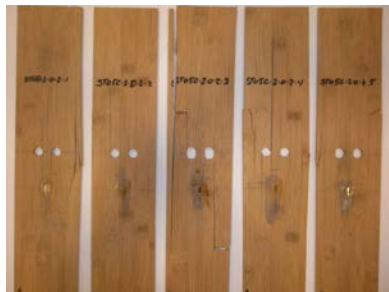
Geometry	Width	Thickness	Max Load	Max Stress	Max Strain
OB	(in)	(in)	(lbf)	(psi)	(in/in)
1	3.52	0.24	8323	11475	4959
2	3.53	0.24	7500	10365	4948
3	3.52	0.24	9568	13291	6736
4	-	-	-	-	-
5	-	-	-	-	-
Mean	3.52	0.24	8464	11710	5548
COV	0.00	0.01	0.12	0.13	0.19

Geometry	OC		
Batch	1	Natural	
No. of holes	N	2	-
Diameter of holes	h	0.50	in
Hole gage	g	1.00	in
Hole spacing	s	0.00	in
Leading edge	L <sub>c</sub>	-	in




Geometry	Width	Thickness	Max Load	Max Stress	Max Strain
OC	(in)	(in)	(lbf)	(psi)	(in/in)
1	3.53	0.24	9284	15114	5316
2	3.54	0.25	8643	13846	5606
3	3.53	0.25	8426	13575	4560
4	3.54	0.24	9442	15230	4907
5	3.53	0.25	9087	14548	4057
Mean	3.53	0.24	8976	14463	4889
COV	0.00	0.01	0.05	0.05	0.13

Geometry	OC		
Batch	1	Caramelized	
No. of holes	N	2	-
Diameter of holes	h	0.50	in
Hole gage	g	1.00	in
Hole spacing	s	0.00	in
Leading edge	L <sub>c</sub>	-	in




Geometry	Width	Thickness	Max Load	Max Stress	Max Strain
OC	(in)	(in)	(lbf)	(psi)	(in/in)
1	3.52	0.24	8443	13968	12452
2	3.51	0.24	7623	12910	5420
3	3.52	0.24	7005	11619	5168
4	3.51	0.24	7492	12633	6922
5	3.52	0.24	6919	11473	4023
Mean	3.51	0.24	7260	12159	5383
COV	0.00	0.01	0.05	0.06	0.22

Geometry	OD		
Batch	1	Natural	
No. of holes	N	2	-
Diameter of holes	h	0.50	in
Hole gage	g	2.00	in
Hole spacing	s	0.00	in
Leading edge	L <sub>c</sub>	-	in




Geometry	Width	Thickness	Max Load	Max Stress	Max Strain
OD	(in)	(in)	(lbf)	(psi)	(in/in)
1	3.52	0.24	8094	13327	7709
2	3.50	0.24	8120	13276	7146
3	3.51	0.24	8021	13119	7443
4	3.51	0.25	7363	11908	7722
5	3.52	0.24	8371	13647	7035
Mean	3.51	0.24	7994	13055	7411
COV	0.00	0.01	0.05	0.05	0.04

Geometry	OD		
Batch	1	Caramelized	
No. of holes	N	2	-
Diameter of holes	h	0.50	in
Hole gage	g	2.00	in
Hole spacing	s	0.00	in
Leading edge	L <sub>c</sub>	-	in




Geometry	Width	Thickness	Max Load	Max Stress	Max Strain
OD	(in)	(in)	(lbf)	(psi)	(in/in)
1	3.54	0.24	5080	8513	4687
2	3.53	0.24	7838	13076	7036
3	3.53	0.24	6783	11245	7542
4	3.53	0.24	7865	13043	6452
5	3.54	0.24	6355	10511	6727
Mean	3.54	0.24	6784	11278	6489
COV	0.00	0.01	0.17	0.17	0.17

Geometry	OJ		
Batch	1	Natural	
No. of holes	N	3	-
Diameter of holes	h	0.50	in
Hole gage	g	1.00	in
Hole spacing	s	0.00	in
Leading edge	L <sub>c</sub>	-	in



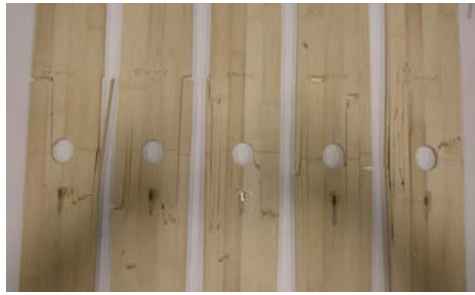
Geometry	Width	Thickness	Max Load	Max Stress	Max Strain
OJ	(in)	(in)	(lbf)	(psi)	(in/in)
1	3.51	0.25	6447	13045	5180
2	3.52	0.25	7609	15334	5041
3	3.53	0.24	7438	14990	5051
4	3.52	0.25	7172	14339	4825
5	3.52	0.25	6696	13401	5608
Mean	3.52	0.25	7072	14222	5141
COV	0.00	0.00	0.07	0.07	0.06

Geometry	OJ		
Batch	1	Caramelized	
No. of holes	N	3	-
Diameter of holes	h	0.50	in
Hole gage	g	1.00	in
Hole spacing	s	0.00	in
Leading edge	L <sub>c</sub>	-	in




Geometry	Width	Thickness	Max Load	Max Stress	Max Strain
OJ	(in)	(in)	(lbf)	(psi)	(in/in)
1	3.54	0.24	7338	15125	5159
2	3.54	0.24	4267	8596	3291
3	3.54	0.24	6817	13924	4560
4	3.54	0.24	5182	10437	4341
5	3.54	0.24	6275	12936	3750
Mean	3.54	0.24	5976	12204	4220
COV	0.00	0.01	0.21	0.22	0.17

Geometry	OB		
Batch	1	Natural	
No. of holes	N	1	-
Diameter of holes	h	1.00	in
Hole gage	g	0.00	in
Hole spacing	s	0.00	in
Leading edge	L <sub>c</sub>	-	in




Geometry	Width	Thickness	Max Load	Max Stress	Max Strain
OB	(in)	(in)	(lbf)	(psi)	(in/in)
1	3.52	0.25	8650	13877	2271
2	3.53	0.24	6687	10830	2792
3	3.52	0.24	5912	9623	2921
4	3.52	0.24	5997	9719	2654
5	3.52	0.25	5896	9481	2646
Mean	3.52	0.25	6628	10706	2657
COV	0.00	0.01	0.18	0.17	0.09

Geometry	OD		
Batch	1	Natural	
No. of holes	N	2	-
Diameter of holes	h	1.00	in
Hole gage	g	2.00	in
Hole spacing	s	0.00	in
Leading edge	L <sub>c</sub>	-	in



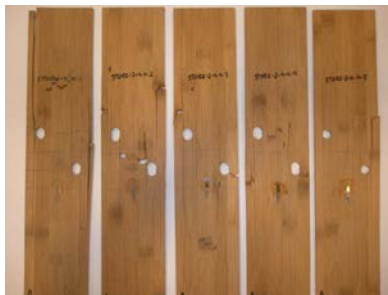
Geometry	Width	Thickness	Max Load	Max Stress	Max Strain
OD	(in)	(in)	(lbf)	(psi)	(in/in)
1	3.52	0.24	3743	10229	3909
2	3.54	0.24	3855	10443	4399
3	3.53	0.24	4210	11479	4919
4	3.52	0.24	4528	12303	4236
5	3.53	0.25	4787	12779	3937
Mean	3.53	0.24	4225	11446	4280
COV	0.00	0.01	0.10	0.10	0.10

Geometry	OE		
Batch	1	Caramelized	
No. of holes	N	2	-
Diameter of holes	h	0.50	in
Hole gage	g	1.00	in
Hole spacing	s	2.00	in
Leading edge	L <sub>c</sub>	-	in




Geometry	Width	Thickness	Max Load	Max Stress	Max Strain
OE	(in)	(in)	(lbf)	(psi)	(in/in)
1	3.50	0.24	8596	14301	7590
2	3.52	0.24	8856	14711	10434
3	3.52	0.24	8258	13456	5818
4	3.51	0.24	6856	11276	6750
5	3.52	0.24	8497	14090	7389
Mean	3.51	0.24	8213	13567	7596
COV	0.00	0.01	0.10	0.10	0.23

Geometry	OF		
Batch	1	Caramelized	
No. of holes	N	2	-
Diameter of holes	h	0.50	in
Hole gage	g	2.00	in
Hole spacing	s	2.00	in
Leading edge	L <sub>c</sub>	-	in




Geometry	Width	Thickness	Max Load	Max Stress	Max Strain
OF	(in)	(in)	(lbf)	(psi)	(in/in)
1	3.52	0.24	7932	13034	8157
2	3.51	0.24	7766	13062	6043
3	3.52	0.24	7475	12239	6464
4	3.51	0.24	7229	11942	6516
5	3.52	0.26	7467	11539	6234
Mean	3.52	0.24	7574	12363	6683
COV	0.00	0.03	0.04	0.05	0.13

Geometry	OG		
Batch	1	Caramelized	
No. of holes	N	2	-
Diameter of holes	h	0.50	in
Hole gage	g	2.00	in
Hole spacing	s	1.00	in
Leading edge	L <sub>c</sub>	-	in




Geometry	Width	Thickness	Max Load	Max Stress	Max Strain
OG	(in)	(in)	(lbf)	(psi)	(in/in)
1	3.52	0.24	7502	12193	6205
2	3.52	0.24	6615	10869	5766
3	3.50	0.24	9131	14859	8028
4	3.52	0.24	7119	11739	6922
5	3.49	0.24	8046	13417	7495
Mean	3.51	0.24	7682	12616	6883
COV	0.00	0.01	0.13	0.12	0.13

Geometry	OH		
Batch	1	Caramelized	
No. of holes	N	2	-
Diameter of holes	h	0.50	in
Hole gage	g	1.00	in
Hole spacing	s	1.00	in
Leading edge	L <sub>c</sub>	-	in




Geometry	Width	Thickness	Max Load	Max Stress	Max Strain
OH	(in)	(in)	(lbf)	(psi)	(in/in)
1	3.52	0.24	7318	12214	5773
2	3.52	0.24	6597	10987	4907
3	3.52	0.24	6954	11523	4917
4	3.51	0.23	6676	11611	5352
5	3.52	0.24	7375	12207	5021
Mean	3.52	0.24	6984	11709	5194
COV	0.00	0.02	0.05	0.04	0.07

Geometry	OK		
Batch	1	Caramelized	
No. of holes	N	3	-
Diameter of holes	h	0.50	in
Hole gage	g	0.50	in
Hole spacing	s	1.00	in
Leading edge	L <sub>c</sub>	-	in



Geometry	Width	Thickness	Max Load	Max Stress	Max Strain
OK	(in)	(in)	(lbf)	(psi)	(in/in)
1	3.49	0.24	5031	10610	3022
2	3.51	0.24	5154	10742	2761
3	3.50	0.24	5106	10750	3371
4	3.50	0.24	4638	9480	2538
5	3.50	0.24	4586	9633	2464
Mean	3.50	0.24	4903	10243	2831
COV	0.00	0.01	0.06	0.06	0.13


Geometry	OL		
Batch	1	Caramelized	
No. of holes	N	3	-
Diameter of holes	h	0.50	in
Hole gage	g	1.00	in
Hole spacing	s	1.00	in
Leading edge	L <sub>c</sub>	-	in



Geometry	Width	Thickness	Max Load	Max Stress	Max Strain
OL	(in)	(in)	(lbf)	(psi)	(in/in)
1	3.50	0.24	6277	13132	4860
2	3.47	0.24	5177	10893	4790
3	3.50	0.24	6622	13846	5726
4	3.49	0.23	4855	10558	4209
5	3.49	0.24	5131	10872	4808
Mean	3.49	0.24	5612	11860	4879
COV	0.00	0.02	0.14	0.13	0.11




Geometry	OM		
Batch	1	Caramelized	
No. of holes	N	3	-
Diameter of holes	h	0.50	in
Hole gage	g	0.50	in
Hole spacing	s	2.00	in
Leading edge	L <sub>c</sub>	-	in



Geometry	Width	Thickness	Max Load	Max Stress	Max Strain
OM	(in)	(in)	(lbf)	(psi)	(in/in)
1	3.53	0.24	5924	12287	4825
2	3.53	0.24	6283	12907	5706
3	3.53	0.24	6312	12838	6004
4	3.54	0.24	5317	10931	6209
5	3.53	0.24	5921	12220	5485
Mean	3.53	0.24	5951	12236	5646
COV	0.00	0.01	0.07	0.06	0.09

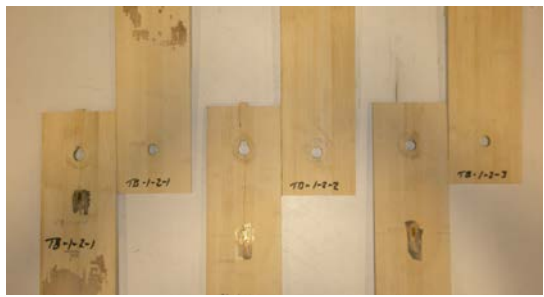
Geometry	ON		
Batch	1	Caramelized	
No. of holes	N	3	-
Diameter of holes	h	0.50	in
Hole gage	g	1.00	in
Hole spacing	s	2.00	in
Leading edge	L <sub>c</sub>	-	in



Geometry	Width	Thickness	Max Load	Max Stress	Max Strain
ON	(in)	(in)	(lbf)	(psi)	(in/in)
1	3.52	0.24	7264	15077	6578
2	3.51	0.25	6898	13951	6104
3	3.52	0.24	6750	13942	5698
4	3.51	0.24	7112	14484	6264
5	3.52	0.24	7641	15713	6892
Mean	3.52	0.24	7133	14634	6307
COV	0.00	0.01	0.05	0.05	0.07


#### A.4 SINGLE GAGE BOLTED LAP-SPLICE TESTS

Geometry	BB		
Batch	1	Natural	
No. of holes	N	1	-
Diameter of holes	h	0.50	in
Hole gage	g	0.00	in
Hole spacing	s	0.00	in
Leading edge	L <sub>c</sub>	2.00	in



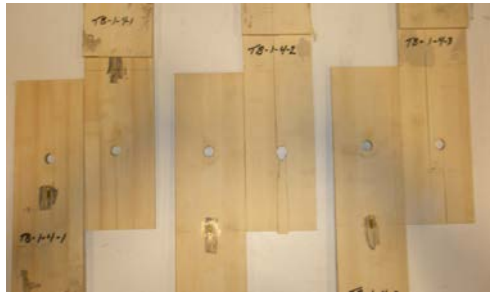
Geometry	Width	Thickness	Max Load	Max Stress	Max Strain
BB	(in)	(in)	(lbf)	(psi)	(in/in)
1	3.42	0.24	1414	2011	938
2	3.41	0.25	1622	2262	1305
3	3.41	0.24	1629	2306	1208
Mean	3.42	0.24	1555	2193	1150
COV	0.00	0.01	0.08	0.07	0.17

Geometry	BB		
Batch	1	Natural	
No. of holes	N	1	-
Diameter of holes	h	1.00	in
Hole gage	g	0.00	in
Hole spacing	s	0.00	in
Leading edge	L <sub>c</sub>	2.00	in




Geometry	Width	Thickness	Max Load	Max Stress	Max Strain
BB	(in)	(in)	(lbf)	(psi)	(in/in)
1	3.41	0.24	1628	2760	483
2	3.41	0.24	988	1698	721
3	3.42	0.24	1456	2501	955
Mean	3.41	0.24	1357	2320	720
COV	0.00	0.01	0.24	0.24	0.33

Geometry	BC		
Batch	1	Natural	
No. of holes	N	1	-
Diameter of holes	h	0.50	in
Hole gage	g	0.00	in
Hole spacing	s	0.00	in
Leading edge	L <sub>c</sub>	4.00	in




Geometry	Width	Thickness	Max Load	Max Stress	Max Strain
BC	(in)	(in)	(lbf)	(psi)	(in/in)
1	3.42	0.25	1652	2321	337
2	3.42	0.25	1883	2610	1021
3	3.42	0.26	1743	2399	1138
Mean	3.42	0.25	1759	2443	832
COV	0.00	0.02	0.07	0.06	0.52

Geometry	BC		
Batch	1	Natural	
No. of holes	N	1	-
Diameter of holes	h	1.00	in
Hole gage	g	0.00	in
Hole spacing	s	0.00	in
Leading edge	L <sub>c</sub>	4.00	in




Geometry	Width	Thickness	Max Load	Max Stress	Max Strain
BC	(in)	(in)	(lbf)	(psi)	(in/in)
1	3.42	0.25	1903	3202	1240
2	3.42	0.25	1659	2782	971
3	3.41	0.25	2121	3555	1538
Mean	3.41	0.25	1894	3179	1250
COV	0.00	0.00	0.12	0.12	0.23

Geometry	BD		
Batch	1	Natural	
No. of holes	N	1	-
Diameter of holes	h	0.50	in
Hole gage	g	0.00	in
Hole spacing	s	0.00	in
Leading edge	L <sub>c</sub>	6.00	in



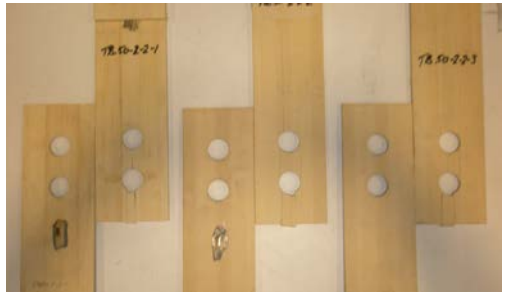
Geometry	Width	Thickness	Max Load	Max Stress	Max Strain
BD	(in)	(in)	(lbf)	(psi)	(in/in)
1	3.52	0.25	2002	2747	902
2	3.51	0.25	1829	2457	820
3	3.52	0.25	2014	2757	993
Mean	3.51	0.25	1948	2654	905
COV	0.00	0.00	0.05	0.06	0.10

Geometry	BE		
Batch	1	Natural	
No. of holes	N	2	-
Diameter of holes	h	0.50	in
Hole gage	g	0.00	in
Hole spacing	s	2.00	in
Leading edge	L <sub>c</sub>	2.00	in




Geometry	Width	Thickness	Max Load	Max Stress	Max Strain
BE	(in)	(in)	(lbf)	(psi)	(in/in)
1	3.42	0.24	2597	3622	1792
2	3.43	0.24	1979	2805	1797
3	3.41	0.25	2634	3676	1728
Mean	3.42	0.24	2404	3368	1772
COV	0.00	0.01	0.15	0.14	0.02

Geometry	BE		
Batch	1	Natural	
No. of holes	N	2	-
Diameter of holes	h	1.00	in
Hole gage	g	0.00	in
Hole spacing	s	2.00	in
Leading edge	L <sub>c</sub>	2.00	in




Geometry	Width	Thickness	Max Load	Max Stress	Max Strain
BE	(in)	(in)	(lbf)	(psi)	(in/in)
1	3.42	0.25	2692	4517	1631
2	3.42	0.24	2770	4689	1797
3	3.42	0.25	2955	4913	2105
Mean	3.42	0.25	2806	4706	1844
COV	0.00	0.01	0.05	0.04	0.13

Geometry	BF		
Batch	1	Natural	
No. of holes	N	2	-
Diameter of holes	h	0.50	in
Hole gage	g	0.00	in
Hole spacing	s	4.00	in
Leading edge	L <sub>c</sub>	4.00	in




Geometry	Width	Thickness	Max Load	Max Stress	Max Strain
BF	(in)	(in)	(lbf)	(psi)	(in/in)
1	3.49	0.24	3068	4185	2010
2	3.50	0.24	3010	4177	2828
3	3.51	0.24	3025	4223	2446
Mean	3.50	0.24	3034	4195	2428
COV	0.00	0.00	0.01	0.01	0.17

Geometry	BG		
Batch	1	Natural	
No. of holes	N	2	-
Diameter of holes	h	0.50	in
Hole gage	g	0.00	in
Hole spacing	s	4.00	in
Leading edge	L <sub>c</sub>	2.00	in




Geometry	Width	Thickness	Max Load	Max Stress	Max Strain
BG	(in)	(in)	(lbf)	(psi)	(in/in)
1	3.51	0.25	3649	4958	2370
2	3.52	0.25	3414	4636	2063
3	3.52	0.25	3575	4868	2378
Mean	3.52	0.25	3546	4821	2270
COV	0.00	0.01	0.03	0.03	0.08

Geometry	BH		
Batch	1	Natural	
No. of holes	N	2	-
Diameter of holes	h	0.50	in
Hole gage	g	0.00	in
Hole spacing	s	6.00	in
Leading edge	L <sub>c</sub>	2.00	in




Geometry	Width	Thickness	Max Load	Max Stress	Max Strain
BH	(in)	(in)	(lbf)	(psi)	(in/in)
1	3.50	0.25	3003	4118	2101
2	3.52	0.25	3426	4604	2630
3	3.51	0.25	3108	4178	2290
Mean	3.51	0.25	3179	4300	2340
COV	0.00	0.00	0.07	0.06	0.11

Geometry	BJ		
Batch	1	Natural	
No. of holes	N	3	-
Diameter of holes	h	0.50	in
Hole gage	g	0.00	in
Hole spacing	s	2.00	in
Leading edge	L <sub>c</sub>	2.00	in



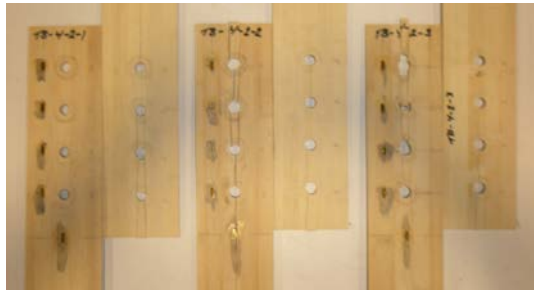
Geometry	Width	Thickness	Max Load	Max Stress	Max Strain
BJ	(in)	(in)	(lbf)	(psi)	(in/in)
1	3.51	0.24	3574	4941	3071
2	3.51	0.24	4273	5892	3298
3	3.51	0.24	4337	5970	2971
Mean	3.51	0.24	4061	5601	3113
COV	0.00	0.00	0.10	0.10	0.05

Geometry	BK		
Batch	1	Natural	
No. of holes	N	3	-
Diameter of holes	h	0.50	in
Hole gage	g	0.00	in
Hole spacing	s	4.00	in
Leading edge	L <sub>c</sub>	4.00	in



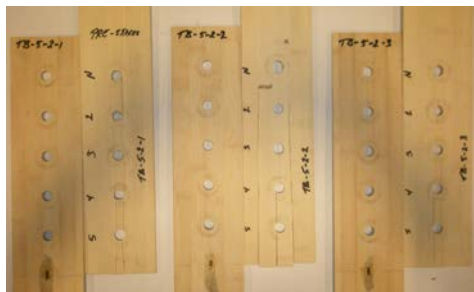
Geometry	Width	Thickness	Max Load	Max Stress	Max Strain
BK	(in)	(in)	(lbf)	(psi)	(in/in)
1	3.52	0.25	5234	7060	3410
2	3.51	0.24	5717	7761	4240
3	3.52	0.24	5201	7079	4124
Mean	3.52	0.24	5384	7300	3925
COV	0.00	0.00	0.05	0.05	0.11

Geometry	BL		
Batch	1	Natural	
No. of holes	N	4	-
Diameter of holes	h	0.50	in
Hole gage	g	0.00	in
Hole spacing	s	2.00	in
Leading edge	L <sub>c</sub>	2.00	in



Geometry	Width	Thickness	Max Load	Max Stress	Max Strain
BL	(in)	(in)	(lbf)	(psi)	(in/in)
1	3.50	0.24	4958	6786	3337
2	3.50	0.24	5121	6997	3192
3	3.50	0.24	6003	8284	4173
Mean	3.50	0.24	5361	7356	3567
COV	0.00	0.00	0.10	0.11	0.15

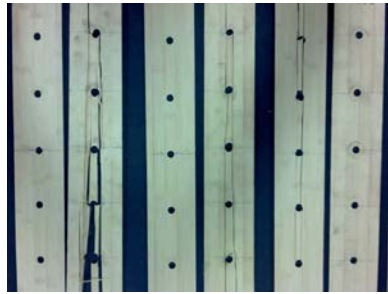
Geometry	BM		
Batch	1	Natural	
No. of holes	N	5	-
Diameter of holes	h	0.50	in
Hole gage	g	0.00	in
Hole spacing	s	2.00	in
Leading edge	L <sub>c</sub>	2.00	in



Geometry	Width	Thickness	Max Load	Max Stress	Max Strain
BM	(in)	(in)	(lbf)	(psi)	(in/in)
1	3.51	0.24	6736	9073	4671
2	3.51	0.24	6496	8730	5593
3	3.51	0.24	7145	9532	5359
Mean	3.51	0.24	6793	9112	5208
COV	0.00	0.01	0.05	0.04	0.09

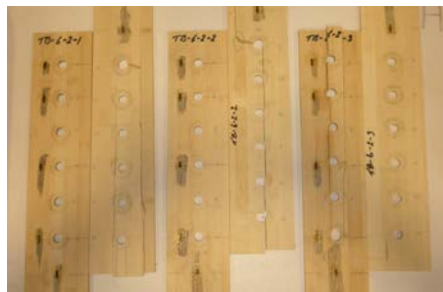


Geometry	BN		
Batch	1	Natural	
No. of holes	N	5	-
Diameter of holes	h	0.50	in
Hole gage	g	0.00	in
Hole spacing	s	4.00	in
Leading edge	L <sub>c</sub>	4.00	in



Geometry	Width	Thickness	Max Load	Max Stress	Max Strain
BN	(in)	(in)	(lbf)	(psi)	(in/in)
1	3.51	0.24	7015	9413	-
2	3.52	0.25	6803	7818	-
3	3.52	0.24	6567	7672	-
Mean	3.52	0.25	6795	8301	-
COV	0.00	0.01	0.03	0.12	-

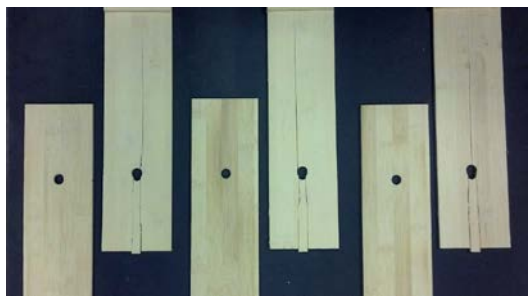
Geometry	BP		
Batch	1	Natural	
No. of holes	N	6	-
Diameter of holes	h	0.50	in
Hole gage	g	0.00	in
Hole spacing	s	2.00	in
Leading edge	L <sub>c</sub>	2.00	in



Geometry	Width	Thickness	Max Load	Max Stress	Max Strain
BP	(in)	(in)	(lbf)	(psi)	(in/in)
1	3.51	0.24	6052	8045	4809
2	3.51	0.25	5388	7207	3882
3	3.51	0.25	8073	10875	5156
Mean	3.51	0.25	6504	8709	4616
COV	0.00	0.01	0.22	0.22	0.14


## A.5 MULTIPLE GAGE BOLTED LAP-SPLICE TESTS

Geometry	SB		
Batch	2	Natural	
No. of holes	N	1	-
Diameter of holes	h	0.50	in
Hole gage	g	0.00	in
Hole spacing	s	0.00	in
Leading edge	L <sub>c</sub>	4.00	in



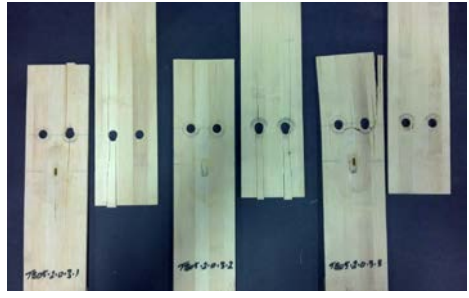
Geometry	Width	Thickness	Max Load	Max Stress	Max Strain
SB	(in)	(in)	(lbf)	(psi)	(in/in)
1	3.50	0.24	1730	1977	-
2	3.50	0.24	1571	1795	-
3	3.50	0.24	1571	1795	-
Mean	3.50	0.24	1624	1856	-
COV	0.00	0.00	0.06	0.06	-

Geometry	SC		
Batch	2	Natural	
No. of holes	N	2	-
Diameter of holes	h	0.50	in
Hole gage	g	1.00	in
Hole spacing	s	0.00	in
Leading edge	L <sub>c</sub>	4.00	in



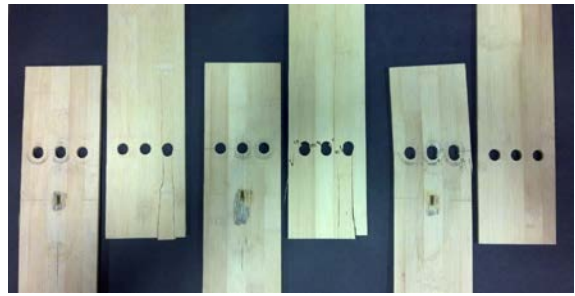
Geometry	Width	Thickness	Max Load	Max Stress	Max Strain
SC	(in)	(in)	(lbf)	(psi)	(in/in)
1	3.52	0.25	2975	3400	1785
2	3.51	0.25	3410	3897	2111
3	3.52	0.24	3157	3608	1250
Mean	3.52	0.25	3181	3635	1715
COV	0.00	0.01	0.07	0.07	0.25

Geometry	SD		
Batch	2	Natural	
No. of holes	N	2	-
Diameter of holes	h	0.50	in
Hole gage	g	1.50	in
Hole spacing	s	0.00	in
Leading edge	L <sub>c</sub>	4.00	in



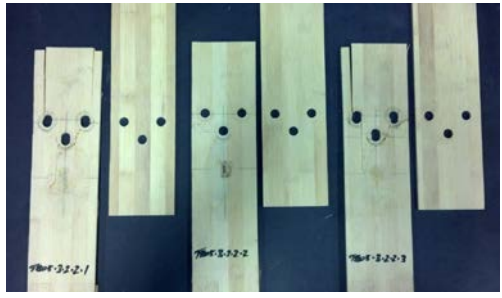
Geometry	Width	Thickness	Max Load	Max Stress	Max Strain
SD	(in)	(in)	(lbf)	(psi)	(in/in)
1	3.50	0.25	3076	3515	-
2	3.52	0.25	3116	3562	-
3	3.51	0.25	3142	3591	-
Mean	3.51	0.25	3111	3556	-
COV	0.00	0.00	0.01	0.01	-

Geometry	SE		
Batch	2	Natural	
No. of holes	N	3	-
Diameter of holes	h	0.50	in
Hole gage	g	1.00	in
Hole spacing	s	0.00	in
Leading edge	L <sub>c</sub>	4.00	in



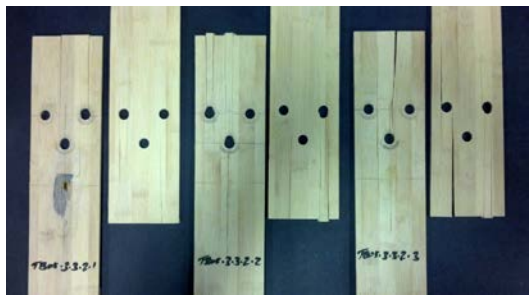
Geometry	Width	Thickness	Max Load	Max Stress	Max Strain
SE	(in)	(in)	(lbf)	(psi)	(in/in)
1	3.51	0.25	4077	4660	-
2	3.52	0.24	3935	4497	-
3	3.52	0.24	4048	4626	-
Mean	3.52	0.24	4020	4594	-
COV	0.00	0.01	0.02	0.02	-

Geometry	SF		
Batch	2	Natural	
No. of holes	N	3	-
Diameter of holes	h	0.50	in
Hole gage	g	1.00	in
Hole spacing	s	1.00	in
Leading edge	L <sub>c</sub>	4.00	in




Geometry	Width	Thickness	Max Load	Max Stress	Max Strain
SF	(in)	(in)	(lbf)	(psi)	(in/in)
1	3.52	0.24	4293	4906	-
2	3.52	0.25	3439	3930	-
3	3.50	0.25	4844	5536	-
Mean	3.51	0.24	4192	4791	-
COV	0.00	0.00	0.17	0.17	-

Geometry	SG		
Batch	2	Natural	
No. of holes	N	3	-
Diameter of holes	h	0.50	in
Hole gage	g	1.00	in
Hole spacing	s	1.50	in
Leading edge	L <sub>c</sub>	4.00	in



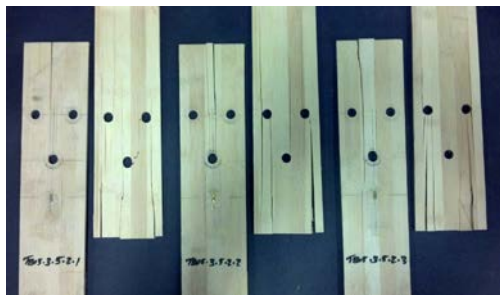
Geometry	Width	Thickness	Max Load	Max Stress	Max Strain
SG	(in)	(in)	(lbf)	(psi)	(in/in)
1	3.51	0.25	5202	5945	-
2	3.51	0.25	4654	5318	-
3	3.52	0.25	4741	5418	-
Mean	3.51	0.25	4865	5560	-
COV	0.00	0.01	0.06	0.06	-

Geometry	SH		
Batch	2	Natural	
No. of holes	N	3	-
Diameter of holes	h	0.50	in
Hole gage	g	1.00	in
Hole spacing	s	2.00	in
Leading edge	L <sub>c</sub>	4.00	in




Geometry	Width	Thickness	Max Load	Max Stress	Max Strain
SH	(in)	(in)	(lbf)	(psi)	(in/in)
1	3.52	0.25	5452	6231	3932
2	3.51	0.24	4876	5573	3767
3	3.51	0.24	5066	5790	4142
Mean	3.51	0.25	5131	5864	3947
COV	0.00	0.01	0.06	0.06	0.05

Geometry	SJ		
Batch	2	Natural	
No. of holes	N	3	-
Diameter of holes	h	0.50	in
Hole gage	g	1.00	in
Hole spacing	s	2.50	in
Leading edge	L <sub>c</sub>	4.00	in



Geometry	Width	Thickness	Max Load	Max Stress	Max Strain
SJ	(in)	(in)	(lbf)	(psi)	(in/in)
1	3.50	0.25	5272	6025	-
2	3.51	0.25	4767	5448	-
3	3.52	0.25	4341	4961	-
Mean	3.51	0.25	4793	5478	-
COV	0.00	0.00	0.10	0.10	-

Geometry	SK		
Batch	2	Natural	
No. of holes	N	3	-
Diameter of holes	h	0.50	in
Hole gage	g	1.00	in
Hole spacing	s	3.00	in
Leading edge	L <sub>c</sub>	4.00	in



Geometry	Width	Thickness	Max Load	Max Stress	Max Strain
SK	(in)	(in)	(lbf)	(psi)	(in/in)
1	3.51	0.25	4769	5450	-
2	3.52	0.24	4382	5007	-
3	3.51	0.25	4843	5534	-
Mean	3.51	0.25	4664	5331	-
COV	0.00	0.01	0.05	0.05	-

## A.6 FLEXURAL TESTS

Bamboo repair plate			
Geometry	A		
Batch	2	Natural	
No. of holes	N	6	-
Width	b	3.50	in
Thickness	t	0.25	in
Diameter of holes	h	0.50	in
Hole gage	g	1.00	in
Hole spacing	s	2.50	in
Leading edge	L <sub>c</sub>	4.00	in

Specimen	Moisture content (%)		Temp.	Depth, d <sub>notch</sub>	Depth, d <sub>beam</sub>	Span	Max Load	Modulus of rupture	Apparent modulus of elasticity	Max Strain <sup>a</sup>	Max Strain <sup>b</sup>
	Beam	Bamboo	(°F)	(in)	(in)	(in)	(lb)	(ksi)	(ksi)	(10 <sup>-6</sup> )	(10 <sup>-6</sup> )
Ca-18	14.2		70	0.00	5.47	54	12958	3225	6.83		
Cb-18	13.3		70	0.00	5.40	54	13588	4007	7.39	7827	
Ca	16.4		70	0.00	5.47	108	6580	4958	8.61		
Cb	14.6		70	0.00	5.47	108	5892	7499	7.78		
CNa	12.4		70	3.48	5.52	108	2162	11625	7.06		
CNb	13.4		70	3.48	5.52	108	1319	10345	4.34	2976	1921
BNa	12.6	10.5	70	3.45	5.48	108	2274	15087	8.44	4771	4999
BNb	12.2	10.5	70	3.43	5.44	108	2339	14024	8.87	5100	
BNSa	12.7	10.5	70	3.48	5.44	108	1703	8926	5.58	4322	
BNSb	14.0	10.5	70	3.45	5.46	108	2381	11841	7.90	5006	

<sup>a</sup>Strain measured at extreme fiber, <sup>b</sup>Strain measured at the surface of the notch

BNSa	
BNSb	
BNa	
BNb	
CNa	
CNb	
Ca	
Cb	

## BIBLIOGRAPHY

- ACI. (2006). *ACI 440.1: Guide for the Design and Construction of Structural Concrete Reinforced with FRP Bars*, Detroit, MI: American Concrete Institute.
- ACI (2008), *ACI 440.2R-08 Guide for the Design and Construction of Externally Bonded FRP Systems for Strengthening of Concrete Structures*, American Concrete Institute, Farmington Hills, MI, USA.
- Aghayere, A., & Vigil, J. (2007). *Structural wood design*. Hoboken, N.J.: John Wiley.
- Ahmad, M. and Kamke, F.A. (2005). “Analysis of Calcutta bamboo for structural composite materials: physical and mechanical properties.” *Wood Science and Technology*, 39(6), 448-459.
- AISC (2010), . *ANSI/AISC 360-10 Specification for Structural Steel Buildings*. American Institute for Steel Construction, Chicago, IL.
- Arce-Villalobos, O.A. (1993). “Fundamentals of the design of bamboo structures.” Master’s Thesis, *Eindhoven University of Technology*, Netherlands.
- Aschheim, M., Gil-Martín, L., & Hernández-Montes, E. (2010). Engineered Bamboo I-Joists. *Journal Of Structural Engineering*, 136(12), 1619-1624. [http://dx.doi.org/10.1061/\(asce\)st.1943-541x.0000235](http://dx.doi.org/10.1061/(asce)st.1943-541x.0000235)
- ASTM International, (2014). *ASTM D143-14: , Standard Test Methods for Small Clear Specimens of Timber*, West Conshohocken, PA: ASTM International.
- ASTM International, (2014). *ASTM D198-14: , Standard Test Methods of Static Tests of Lumber in Structural Sizes*, West Conshohocken, PA: ASTM International.
- ASTM International, (2014). *ASTM D245-06 (reapproved 2011): , Standard Practice for Establishing Grades and Related Allowable Properties for Visually Graded Lumber*, West Conshohocken, PA: ASTM International.
- ASTM International, (2011). *ASTM D2555-11: , Standard Practice for Establishing Clear Wood Strength Values*, West Conshohocken, PA: ASTM International.



- ASTM International, (2012). *ASTM D3737-12: , Standard Practice for Establishing Allowable Properties for Structural Glued Laminated Timber (Glulam)*, West Conshohocken, PA: ASTM International.
- ASTM International, (2015). *ASTM D3846-08 (Reapproved 2015): , Standard Test Method for In-Plane Shear Strength of Reinforced Plastics*, West Conshohocken, PA: ASTM International.
- ASTM International, (2013). *ASTM D4761-13: , Standard Test Methods for Mechanical Properties of Lumber and Wood-Base Structural Material*, West Conshohocken, PA: ASTM International.
- ASTM International, (2014). *ASTM D7341-14: , Standard Practice for Establishing Characteristic Values for Flexural Properties of Structural Glued Laminated Timber by Full-Scale Testing*, West Conshohocken, PA: ASTM International.
- ASTM International, (2013). *ASTM D7438-13: , Standard Practice for Field Calibration and Application of Hand-Held Moisture Meters*, West Conshohocken, PA: ASTM International.
- Cardoso, D. (2014). Compressive Strength of Pultruded Glass-Fiber Reinforced Polymer (GFRP) Columns. *PhD Dissertation*, UFRJ/COPPE, Rio de Janeiro.
- Cunningham, D., Harries, K.A. and Bell, A.J. (2015, in press), Open-Hole Tension Capacity of Pultruded GFRP Having Staggered Hole Arrangement, *Engineering Structures*.
- Dixon, P., & Gibson, L. (2014). “The structure and mechanics of Moso bamboo material.” *Journal Of The Royal Society Interface*, 11(99), 20140321-20140321. <http://dx.doi.org/10.1098/rsif.2014.0321>
- Ghavami, K., Bamboo as reinforcement in structural concrete elements (2005). *Cement and Concrete Composites*, 27, 637-649.
- Harries, K.A., Sharma, B., and Richard, M.J. (2012). “Structural use of full culm bamboo: the path to standardization.” *International Journal of Architecture, Engineering and Construction*, 1(2), 66-75.
- ISO (International Organization for Standardization), (2004a). *International Standard ISO 22156:2004 (E), Bamboo – Structural Design*. Geneva, Switzerland: ISO.
- ISO (International Organization for Standardization), (2004b). *International Standard ISO 22157-1:2004 (E), Bamboo – Determination of Physical and Mechanical Properties – Part I: Requirements*. Geneva, Switzerland: ISO.
- ISO (International Organization for Standardization), (2004c). *International Standard ISO 22157-2:2004 (E), Bamboo – Determination of Physical and Mechanical Properties – Part II: Laboratory Manual*. Geneva, Switzerland: ISO.

- Janssen, J. (1981). “Bamboo in building structures”. Doctoral Thesis, *Eindhoven University of Technology*, Netherlands.
- Kretschmann, D. E. (2012). Mechanical properties of wood. *Environments*, 5, 34.
- Li, F., Liu, Y.F., Gou, M., Zhang, R. and Du, J. (2011). Research on Strengthening Mechanism of Bamboo Fiber Concrete under Splitting Tensile Load, *Advanced Materials Research*, 374-377, 1455-1461.
- Mahdavi, M., Clouston, P., & Arwade, S. (2011). Development of Laminated Bamboo Lumber: Review of Processing, Performance, and Economical Considerations. *J. Mater. Civ. Eng.*, 23(7), 1036-1042. [http://dx.doi.org/10.1061/\(asce\)mt.1943-5533.0000253](http://dx.doi.org/10.1061/(asce)mt.1943-5533.0000253)
- NDS (1997). *National Design Specification (NDS) for Wood Construction with Commentary and Supplement: Design Values for Wood Construction*, Washington, DC: American Forest and Paper Association (AF&PA), American Wood Council (AWC).
- Richard, M.J. (2013). “Assessing the performance of bamboo structural components.” Doctoral Dissertation, *University of Pittsburgh*, Pittsburgh, PA.
- Sharma, B. (2010). “Seismic performance of bamboo structures.” Doctoral Dissertation, *University of Pittsburgh*, Pittsburgh, PA.
- Sharma, B., Gatóo, A., Bock, M., & Ramage, M. (2015). Engineered bamboo for structural applications. *Construction And Building Materials*, 81, 66-73. <http://dx.doi.org/10.1016/j.conbuildmat.2015.01.077>
- Sharma, B., Ramage, M., Bock, M., Gatoo, A., & Mulligan, H. (2015). Engineered bamboo: state of the art. *Proceedings Of The ICE - Construction Materials*, 168(2), 57-67. <http://dx.doi.org/10.1680/coma.14.00020>
- United States Department of the Interior (1995), *The Secretary of the interior’s Standards for the Treatment of Historic Properties with Guidelines for Preserving, Rehabilitating, Restoring and Reconstructing Historic Buildings*, National Park Service, Washington, DC. 188 pp.
- Xiao, Y., Shan, B., Chen, G., Zhou, Q., and She L.Y. (2008), Development of a new type of Glulam – Glubam. *Modern Bamboo Structures*, Xiao, Y., Inoue, M., and Paudel S.K., eds., London, UK, 41-47.